Contact Graphs for Disk Packing in the Plane

UROP+ Final Paper, Summer 2020

Naveen Venkat
Mentor: Vishal Patil
Project suggested by: Vishal Patil

September 1, 2020

Abstract

The disk packing problem asks whether it is possible to place a given set of disks onto a given surface without overlap. A useful tool in analyzing these packings is the contact graph of a packing, in which vertices correspond to centers of disks, and edges correspond to tangencies between disks. In this paper, we show that given a planar graph G, it is NP-Hard to determine whether G is the contact graph of a valid disk packing in the plane. In proving this result, we make use of a proof structure to that of Cabello et al. [*Graph Drawing*, 283-294 (2003)].

1 Introduction

The disk packing problem is concerned with placing a given set of disks onto a given surface such that no two disks overlap. The optimization version of this problem, which involves maximizing radius of the disks and/or minimizing the surface's area, has been studied in many different situations, including equal disk packing in a flat torus [11], unequal disk packing in a circle [10], and equal disk packing in a klein bottle [9]. Meanwhile, the decision version of this problem, which simply asks if a given disk packing is possible, is mainly studied from an algorithmic point of view. For example, Morr's Split Packing algorithm generates the packing of a set of disks into a given square, rectangle, or triangle, provided that the total areas of the disks is no more than a constant fraction of the container area [2]. Additionally, some disk packing problems have been shown to be NP-hard, including packing unit disks in a [not neccessarily connected] planar region [5] or packing [not necessarily equal] disks into a square [6].

One valuable tool in disk packing proofs is the contact graph G_P of a disk packing P. The contact graph G_P of a disk packing P contains a vertex corresponding to the center of each disk in P, and an edge between two vertices for each tangency between the corresponding disks in P. Using the contact graph, we are now able to analyze disk packings using results and techniques from graph theory.

More concretely, we apply similar techniques to those used by Cabello et al. [1] in analyzing graph embeddings to examine planar embeddings of disk packing contact graphs. Here, we focus on unit [diameter] disk packings in the plane. We prove the following Theorem:

Theorem. *Given a planar graph G, it is NP-hard to determine if G is the contact graph of a valid unit disk packing in the plane.*

Our proof works by applying a similar reduction structure to that of Cabello et al. in their proof of the NP-hardness of the straight-line embeddability of 3-connected planar graphs with unit edge lengths [1]. However, the reduction gadgets used in our proof are mostly different from those used in this result because of a few key differences between our problems. While our problem also deals with the straight-line embeddability of planar graphs with unit length edges (our disks have unit diameter, so that we have a unit distance between tangent disks' centers), we do not require that the given graph be 3-connected. However, we have additional restrictions in our problem due to the nature of circle geometry. For example, when embedding our contact graph into the plane, we must ensure not only that edges do not cross, but also that non-adjacent vertices are greater unit distance from each other. Additionally, we must ensure that in our embedding, all angles between adjacent edges are at least $60°$, with $60°$ angles only allowed when all three involved vertices are pairwise adjacent (see Figure 1.1 for a concrete example of this).

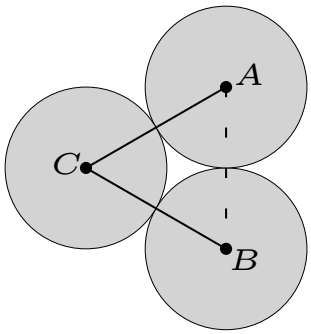

Figure 1.1: Demonstrating the problem constraints. In the figure, disk C is tangent to both disks A and B, so that in the contact graph, vertex C is adjacent to vertices A and B, respectively. By the nature of circle geometry, we cannot have that $m\angle ACB < 60°$. Furthermore, if $m\angle ACB = 60°$, then we must have disks A and B are tangent, which means that vertices A and B must be adjacent in the contact graph.

The outline of our paper is as follows. In Section 2, we discuss some related previous results. Then, in Section 3, we go over some important structures and techniques used in our main proof. In Section 4, we present a Karp-style reduction using a similar structure to [1] to prove our main theorem. And in Appendix A, we analyze the gadgets introduced in the proof to ensure the are realizable within the problem constraints.

2 Previous Results

In this section, we review previous hardness results that relate to the problem at hand.

First, we discuss hardness results proven about disk packing in the plane, without regard to contact graphs. Fowler et al. showed that the problem of whether n unit disks would fit into an arbitrary planar region (not necessarily convex or even connected) is NP-hard, via a reduction from 3SAT [5]. Additionally, Alt et al. showed that the problem of packing n disks onto a 'shelf', that is, placing the disks within a given x-interval such that they do not overlap and each is touching the x-axis from above, is NP-hard [7].

Furthermore, Demaine et al. showed that the problem of packing a given set of disks [of possibly different sizes] into a given square, rectangle, or triangle is NP-hard, via a reduction from 3-partition [6]. This paper also showed NP-hardness for the analogous disk placement problems, in which only the disks' centers (as opposed to the entire disks) are required to fit within the given container.

Related to our problem is the concept of unit disk graphs, intersection graphs for a collection of unit disks that are placed on the plane (that is, graphs for which vertices correspond to the centers of these disks and edges correspond to intersections between two disks). While the two problems differ in their treatment of disks whose placements overlap (whereas such behavior is prohibited in our problem, this simply results in an edge in a unit disk graph), they both contain an edge between vertices that whose corresponding disks are tangent. Breu et al. showed the problem of determining whether a given graph is a unit disk graph is NP-hard [8].

Finally, as previously mentioned, Cabello et al. showed that the problem of determining whether a given planar 3-connected graph is straight-line embeddable with unit edge lengths is NP-hard, even when the graph is known to be rigid [1] [1]. Our proof is heavily inspired by and heavily relies on this result, following nearly the same format for the reduction. However, as our problem slightly differs from that of this result, almost all of our gadgets have been newly constructed to conform to our problem constraints.

[1] A graph is rigid if, when embedding, the relative positions of all vertices are fixed up to rotations and reflections.

3 Preliminaries

In this section, we discuss key structures and techniques used in our reduction.

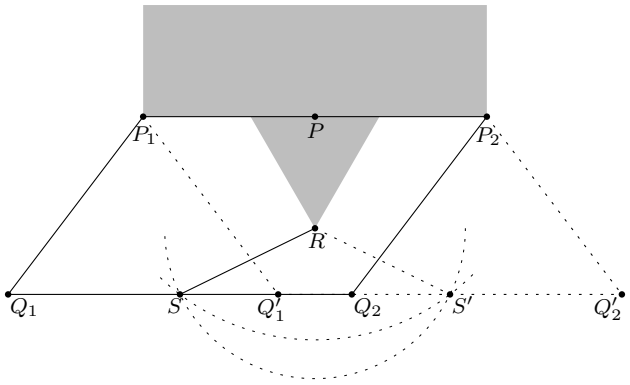

Figure 3.1: The gray structures are fixed and rigid, and black edges are straight. $\overline{Q_1Q_1}$ must be parallel to $\overline{P_1P_2}$, forcing S to lie on a circle with radius PS. But S also lies on an circle with radius $RS \neq PS$. Thus, the entire structure has only two realizations, when S lies at an intersection of the two circles

One structure important to our construction is shown in Figure 3.1. Note that the gray regions are fixed and rigid structures, edges are straight with fixed length, and vertices are free pivots.

First, note that $P_1P_2 = Q_1Q_2$, $P_1Q_1 = P_2Q_2$, P is the midpoint of $\overline{P_1P_2}$, and S is the midpoint of $\overline{Q_1Q_2}$. Then in any realization of this structure, we must have that $\overline{P_1P_2} \parallel \overline{Q_1Q_2}$, so that S must lie on [the arc of] a circle with radius PS (centered at P), which is partially shown. Also, note that $P_1R = P_2R$, with $PR > 0$. Then, because of $\overline{RS}$, S must also lie on [the arc of] a circle with radius $RS \neq PS$ (centered at R), which is partially shown.

Thus, we see that the entire structure has only the two rigid realizations shown, where S is located at the two intersections of these circles. Note that the distance between $\overline{P_1P_2}$ and $\overline{Q_1Q_2}$ is fixed to the same value in either realization.

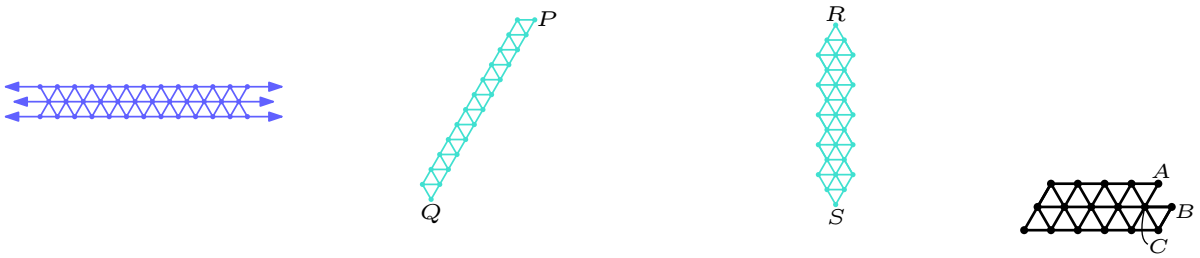

(a) (b) (c) (d)

Figure 3.2: Rigid Triangular Structures (a) A repeating rigid bar structure which we can extend to our preferred length(b) $\overline{PQ}$ simulates an edge of length 12 (c) $\overline{RS}$ simulates an edge of length $6\sqrt{3}$ (d) Such a structure is not allowed within the problem constraints as there would need to be and edge between A and B.

As our problem deals with the contact graphs of disk packings, note that the structures used in our reduction must be graphs. An important technique we use to ensure rigidity of our constructions is the arrangement of vertices into a triangular grid structure. Figures 3.2a-c show some examples of such structures which we use in our proof. Since the triangle grid is a rigid planar structure, the relative positions of all vertices in one of these structures is fixed (up to rotations and reflections). This allows us to create large repeating rigid structures that we can extend to our preferred length, such as the bar in Figure 3.2a. It also allow us to simulate edges of greater than unit length in our graph, such as with $\overline{PQ}$ in Figure 3.2b and $\overline{RS}$ in Figure 3.2c.

Note that all outer angles of these structures must be at least 120°, This is because, in the triangular grid, all angles are multiples of 60°, and, as previously established in our earlier discussion of circle geometry, two disjoint vertices who share a common neighbor must form an angle of greater than 60°. More concretely, a structure like that in Figure 3.2d is not allowed within the problem constraints, since $m\angle ACB = 60°$, but there is no edge between A and B.

4 NP-Hardness

We now get to the main result of the paper, proving the Theorem from Section 1. We begin by providing an overview of how the reduction will be implemented. We then prove the theorem from the introduction. Once again, we mention that our proof is heavily inspired by and heavily relies on the previous result in [1].

Note that the gadgets used in the proof are only introduced and analyzed for their function in this section; the detailed verification of the realizability of these gadgets (within the circle geometry problem constraints established in Section 1) is established in the lemmas in Appendix A. We restate the theorem below for convenience.

Theorem. *Given a planar graph G, it is NP-hard to determine if G is the contact graph of a valid unit disk packing in the plane.*

Sketch of Proof In proving our result, we reduce[2] from Planar Rectilinear 3-Satisfiability (PR3SAT), a variant of Planar 3-Satisfiablity that is also strongly NP-Complete [3][4]. In a PR3SAT instance, we are given a planar bipartite graph, with one set of nodes $v_1, v_2, \ldots, v_n$ representing the variables and the other set of nodes $c_1, c_2, \ldots, c_m$ representing the clauses of a regular 3SAT instance, where each clause node is connected to the three variable nodes whose literals appear in that clause. We are also given that the variables are arranged in a [horizontal] line, that the clauses and their corresponding three edges (each with at most one turn) either lie fully above or fully below this line, and that the entire graph lies on a square grid of polynomial size (as shown in Figure 4.1a).

We begin the reduction by moving this graph to a triangular grid, so that all angles are multiples of 60°, following the proof structure in [1] (as explained in Section 3, this helps us to create rigid structures for our gadgets). We further modify the variable-clause edges so that all angles along the edges are 120°, and the three edges connected to a clause enter at 120° angles to each other (as in Figure 4.1b). Note how, through the way we orient the 'openings' to the clauses above and below and variable line, we force every edge to contain at least one turn.

This 'metagraph' layout is then constructed through a combination of various gadget structures, of similar construction to [1]. Namely, we create rigid tunnel gadgets along the paths of variable-clause edges in this 'metagraph' layout. We also create variable gadgets that have exactly two realizations corresponding to a variable's truth value, rigidly connecting these into a horizontal line. We then have rigid wire gadgets that transmit the value of a literal through the tunnel gadget from the variable gadget to the clause gadget, where each clause gadget is realizable if and only if it contains at least one true literal. For a visualization of this, see Figure 4.1b, in which the black lines correspond to tunnel gadgets, the blue lines correspond to wire gadgets, the variable boxes correspond to variable gadgets, and the clause hexagons correspond to the clause gadgets. □

[2]In a Karp-style reduction, we say that we can reduce from decision problem A to decision problem B if we can demonstrate a polynomial-time algorithm that can convert an instance a of problem A into an instance b of problem B such that b is a positive instance of problem B if and only if a is a positive instance of problem A. Thus, if we know that problem A is NP-hard, and we can reduce from A to B, then we have that problem B is NP-hard.

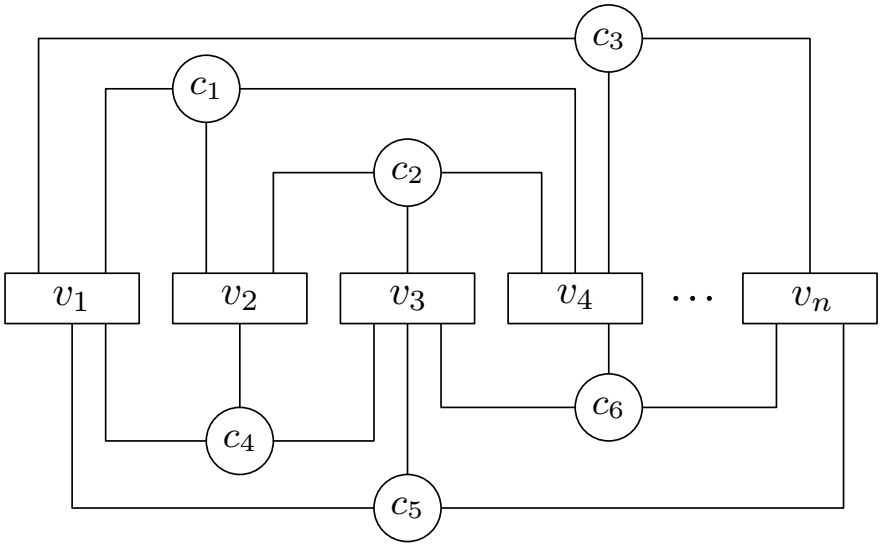

(a)

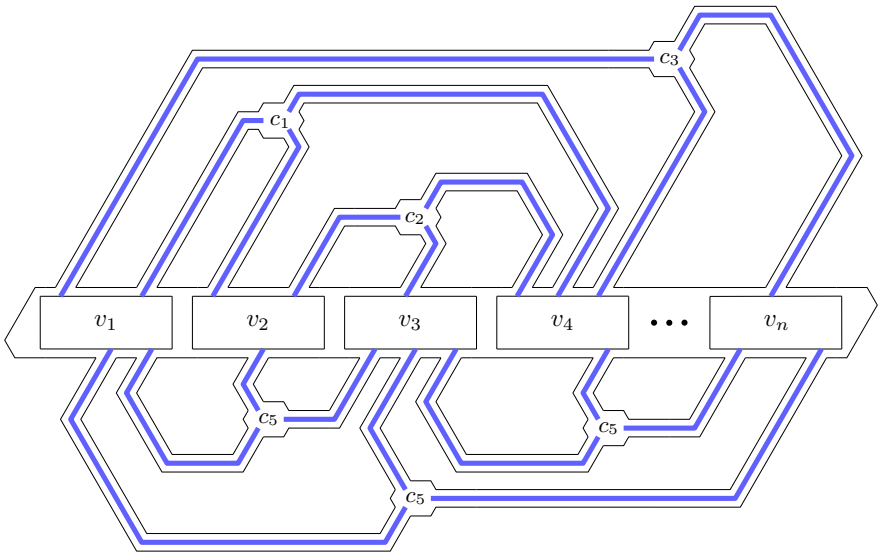

(b)

Figure 4.1: (a) An example planar rectilinear 3-satisfiability instance. The variables can be arranged in a line, with the three-legged clauses and their corresponding edges placed either above or below this line, and the whole graph drawn on a square grid. (b) Following the structure of the reduction from [1], our reduction from this instance starts by moving the graph to a triangular grid.

We now move on to the full proof of the theorem.

Proof. Since we have already described the high-level structure of this reduction, all that remains is for us to demonstrate the gadgets used in the reduction.

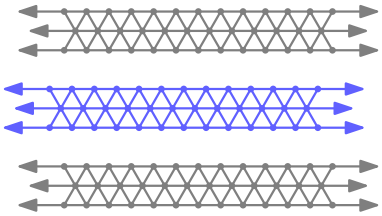

Figure 4.2: The Tunnel Gadget

At the most basic level, our construction relies on wire gadgets that transmit the value of a literal from the variable gadget to the clause gadget, as well as tunnel gadgets that contain these wire gadgets. Figure 4.2 shows a visualization of [a segment of] the tunnel and wire gadgets, where the gray bars make up the tunnel gadget, and the inner blue bar is the wire gadget. As the two are often used together, we sometimes refer to the combination as the tunnel/wire gadget. By Lemma A.1.1, we have that the tunnel/wire gadget is realizable within the problem constraints.

This structure is very similar to the tunnel gadgets in [1], as it is both 3-connected and realizable as a circle packing.

Next, we need a holder gadget to fix the position of the two sides of the tunnel relative to each other, in addition to rigidly holding the wire gadget in place in the middle of the tunnel. As the wire gadget needs to be able to transmit the truth value of a literal, we construct this holder gadget to have two possible configurations. See Figure 4.3 for a visualization of the holder gadget. Figures 4.3a and 4.3b show the desired two realizations of the gadget.

Now, we examine the top half of Figure 4.3a (the bottom half of the gadget is a mirror image of the top half). Specifically, note how $P_1P_2 = Q_1Q_2$, $P_1Q_1 = P_2Q_2$, $P_1R = P_2R$, and S is the midpoint of $\overline{Q_1Q_2}$. Thus, we have that this top half-gadget functions identically to the structure in Figure 3.1, so that it has two possible realizations, and the wire gadget is held at a fixed distance from the side of the tunnel gadget.

Our holder gadget differs quite a lot from that in [1], as we did not need to make the structure 3-connected, while in [1], Cabello et al. did not need to obey our problem's angle constraints. Because of this, the two constructions have different approaches to handling pivots, a pattern which will be seen again in later gadgets.

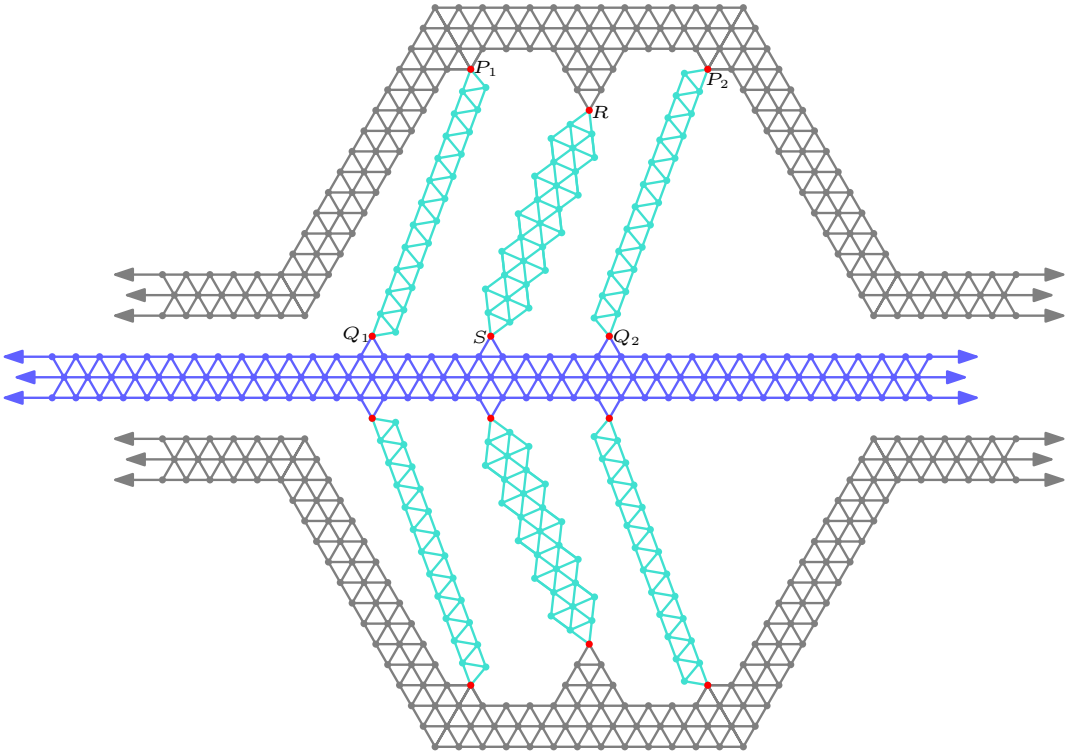

(a)

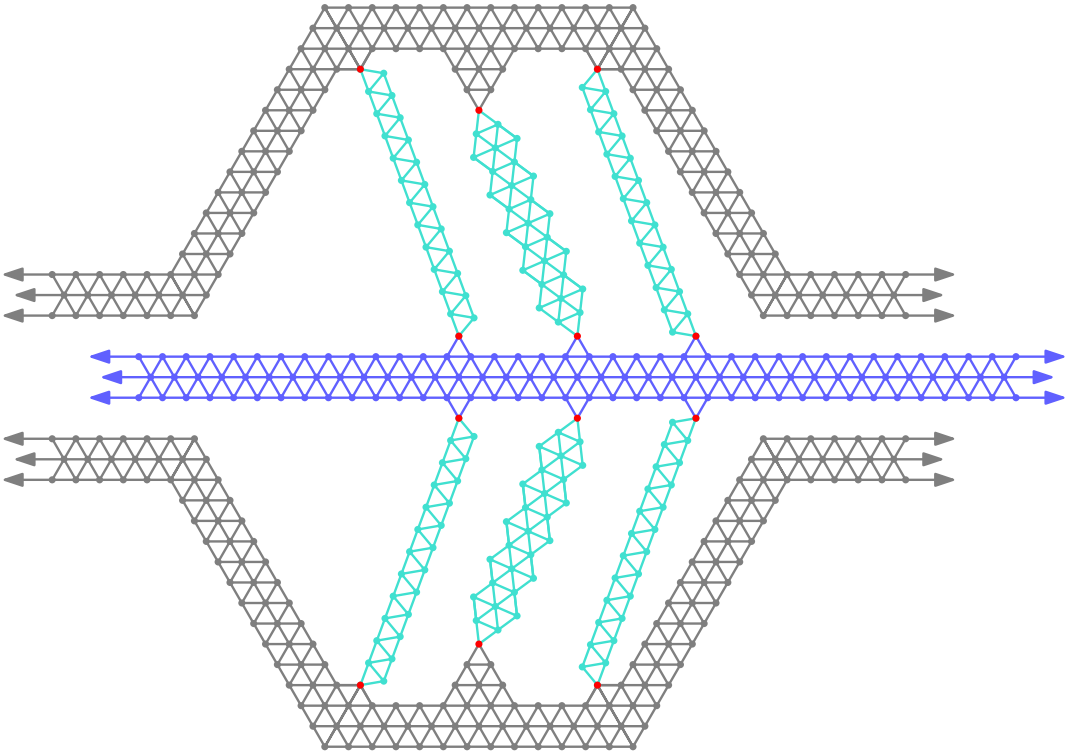

(b)

Figure 4.3: The Holder Gadget. (a) & (b) show the two different desired configurations of the gadget.

Note that while this construction forces a particular embedding for the wire gadget relative to the tunnel gadget, each of the three turquoise structures, which we refer to as "struts", still has two possible planar embeddings, by flipping the entire strut over $\overline{P_1Q_1}$, $\overline{P_2Q_2}$, or $\overline{RS}$, respectively. However, since these alternate embeddings still preserve the lengths P_1Q_1, P_2Q_2, and RS that our construction relies on, the gadget cannot be subverted by use of an alternated embedding of one of these struts. Indeed, these alternate embeddings can only do worse than our suggested embedding by possibly causing the gadget to fail to satisfy the problem constraints in the previously verified configurations in 4.3.

By Lemmas A.2.1 and A.2.5, we have that these two desired configurations are realizable within the problem constraints. We also have, by Corollary A.2.2, that the wire gadget is shifted by $\sqrt{69}$ units between these two configurations. Thus, the wire can transmit information through the direction it is pushed by the holder gadget. We call this directional 'pushing information' of the wire gadget *pressure*. Note that each straight part of the tunnel/wire gadget must contain at least one holder gadget. Note that we sometimes include holder gadgets in our figures of other gadgets to aid in the visualization of the pressure of wires.

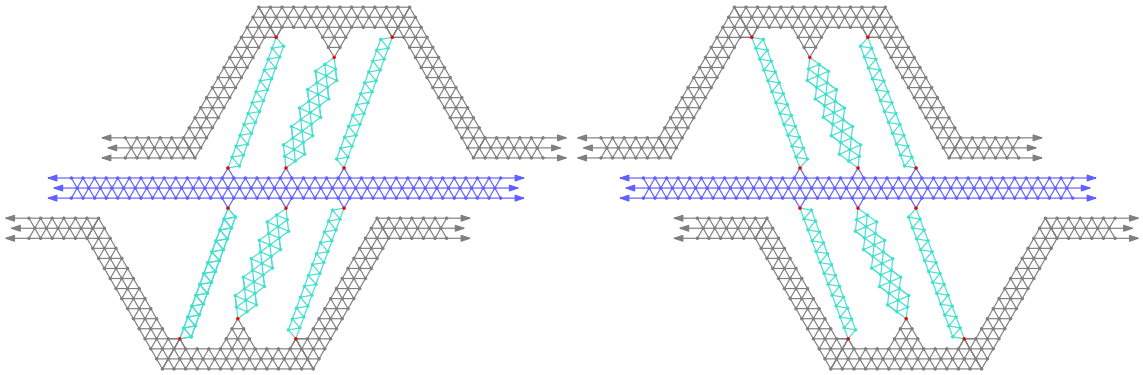

(a) (b)

Figure 4.4: The Misaligned Holder Gadget. (a) & (b) show the two undesired configurations of the holder gadget, in which the sides of the tunnel are misaligned.

However, because each half of the gadget has two possible realizations, this means that the holder gadget has four possible configurations: the two desired configurations in Figures 4.3a and 4.3b, and the two configurations in Figure 4.4 in which the sides of the tunnel become misaligned. It turns out that these configurations are impossible within our construction. But before we can address this, we need to introduce the next gadget: the turn gadget.

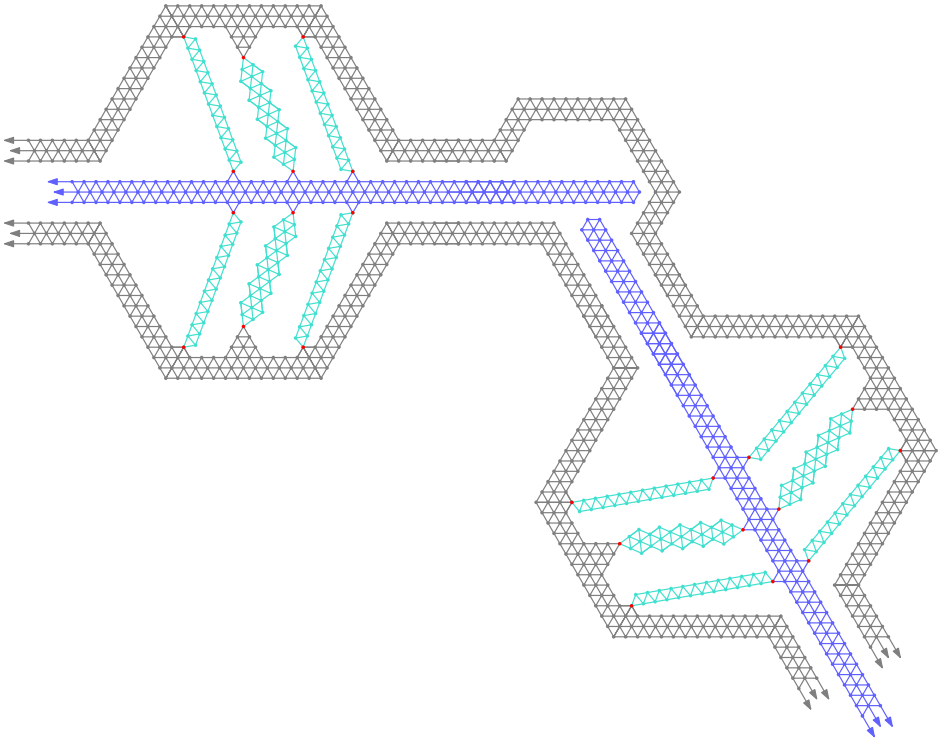

(a)

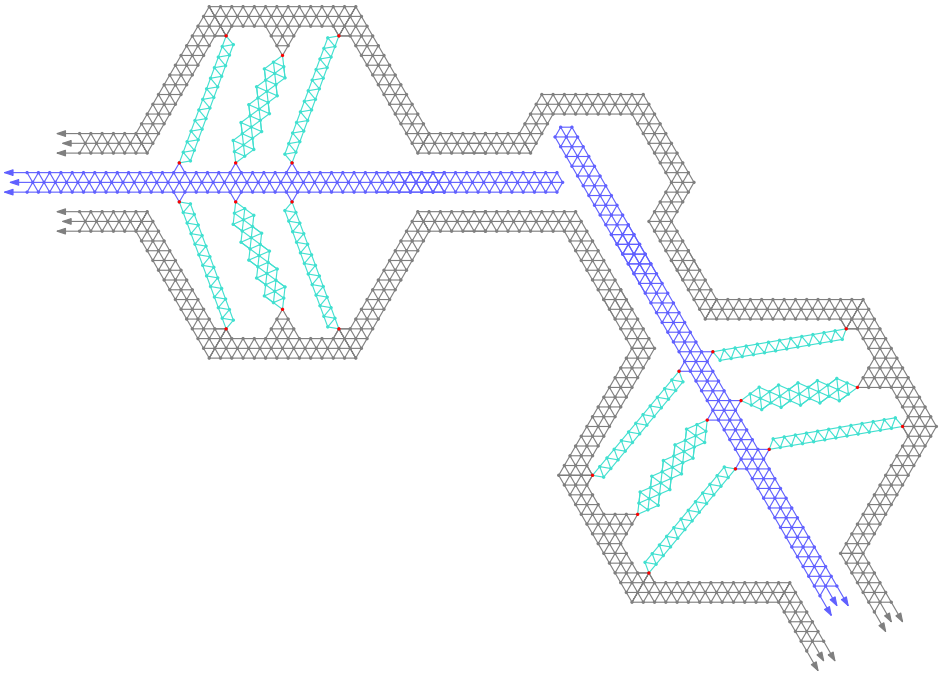

(b)

Figure 4.5: The Turn Gadget. (a) & (b) show the two different desired configurations of the holder gadget, sandwiched between two holder gadgets. Note how these configurations correctly transmit pressure around turns.

See Figure 4.5 for a visualization of the turn gadget being used to concatenate two holder gadgets. The turn gadget is used for each of the turns of the tunnel/wire gadget between the variable gadget and clause gadget, as was shown in Figure 4.1b. As we can see in Figures 4.5a and 4.5b, the turn gadget forces the alignment of the sides of the tunnel gadget for any holder gadget to which it is rigidly connected. This is because, if a misaligned holder gadget were to connect to, say, the left end of the turn gadget, as in Figure 4.6, then because of the non-zero shift between the two sides of the tunnel (by Corollary A.2.2), we would have that the tunnel spacing on the right side of the turn gadget would be incompatible (too wide in Figure 4.6a and too narrow in Figure 4.6b) with the tunnel spacing of a holder gadget connected to that side (recall that we have already established the fixed tunnel spacing of the holder gadget). As the gadget is symmetric, this incompatibility holds for a misaligned holder gadget on the other side, as well.

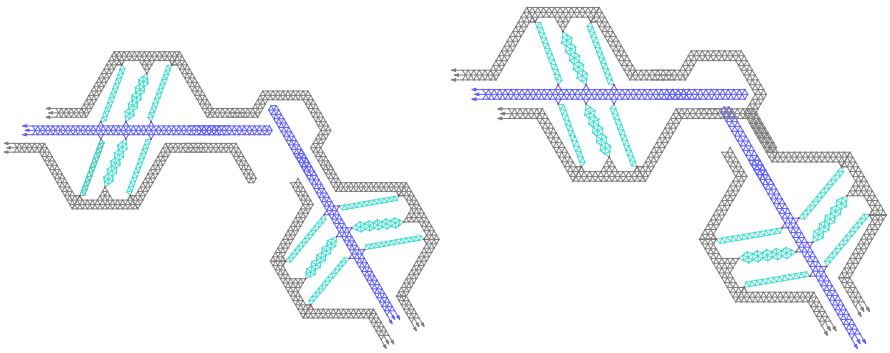

(a) (b)

Figure 4.6: Avoiding the Misaligned Holder Gadget. (a) & (b) Rigidly connecting the holder gadget to the turn gadget prohibits the misaligned configurations of the holder gadget.

Recall that in our construction, we ensured that each tunnel/wire gadget between the variable and clause gadgets contained at least one turn. Thus, we have that every holder gadget is rigidly connected to a turn gadget, so that it is impossible for a misaligned holder gadget to be realized in our construction. Note also that this means the sides of the tunnel gadgets are rigidly connected to each another for each edge in the 'metagraph'. As we will see, the tunnels of adjacent 'metagraph' edges in the variable and clause gadgets are also rigidly connected to each other, so that all tunnel gadgets are connected in a [globally] rigid way.

Let us now return to properly address the turn gadget. Figures 4.5a and 4.5b show the two desired realizations of the gadget (note that the holder gadgets need not be so close to the turn gadget; this is done in the figure for clarity). Note how, in the realizations shown, the turn gadget allows us to correctly transfer pressure around these turns. By Lemma A.3.1, we have that these two desired configurations are realizable within the problem constraints.

Our turn gadget makes use of a similar construction to [1], as it again mainly consists of a triangular grid structure, which is allowed in both problems.

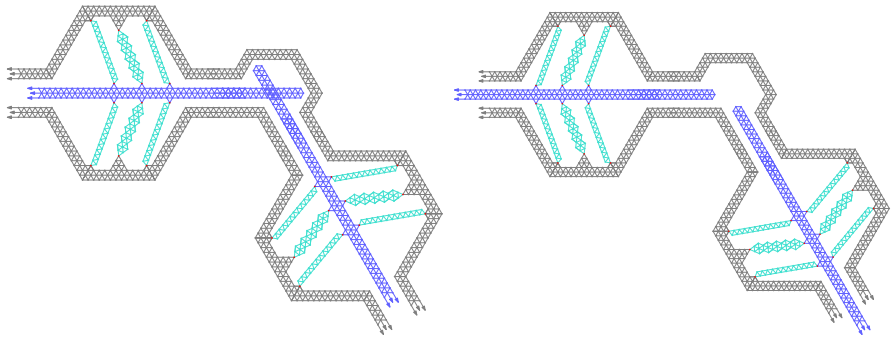

(a) (b)

Figure 4.7: The Undesired Configurations Turn Gadget. (a) This configuration is not realizable within the problem constraints (b) We show that this configuration cannot mess up our construction

However, since each wire end in the gadget has two possible positions, there are also two undesired configurations for the turn gadget, as shown in Figure 4.7, in which the turn gadget does not correctly transmit pressure around the turn. By Lemma A.3.2, we have that the configuration shown in Figure 4.7a is not valid within the problem constraints. Also, it will turn out that the existence of the configuration shown in Figure 4.7b cannot mess up our construction. However, we will need to return to this point after introducing the variable gadget.

Since the variable gadget again needs two possible configurations, we can reuse structures of the holder gadget. As shown in Figure 4.8, the variable gadget consists of a structure similar to the holder gadget on the [left] end, except that instead of a wire gadget, it is connected to a thicker variable bar that extends most of the way through the rest of the gadget (note that the two halves of the modified holder gadget are rigidly connected, so that they cannot misalign). Along the top and bottom of the gadget, the tunnel gadgets for each of this variable's literals are rigidly connected to adjacent tunnel gadgets (note that the holder gadgets for each tunnel need not be so close to the variable gadget; however, this slightly reduces the size of our final graph). In particular, we must make sure to make each variable gadget long enough to accommodate all literals that are connected above and below to the gadget.

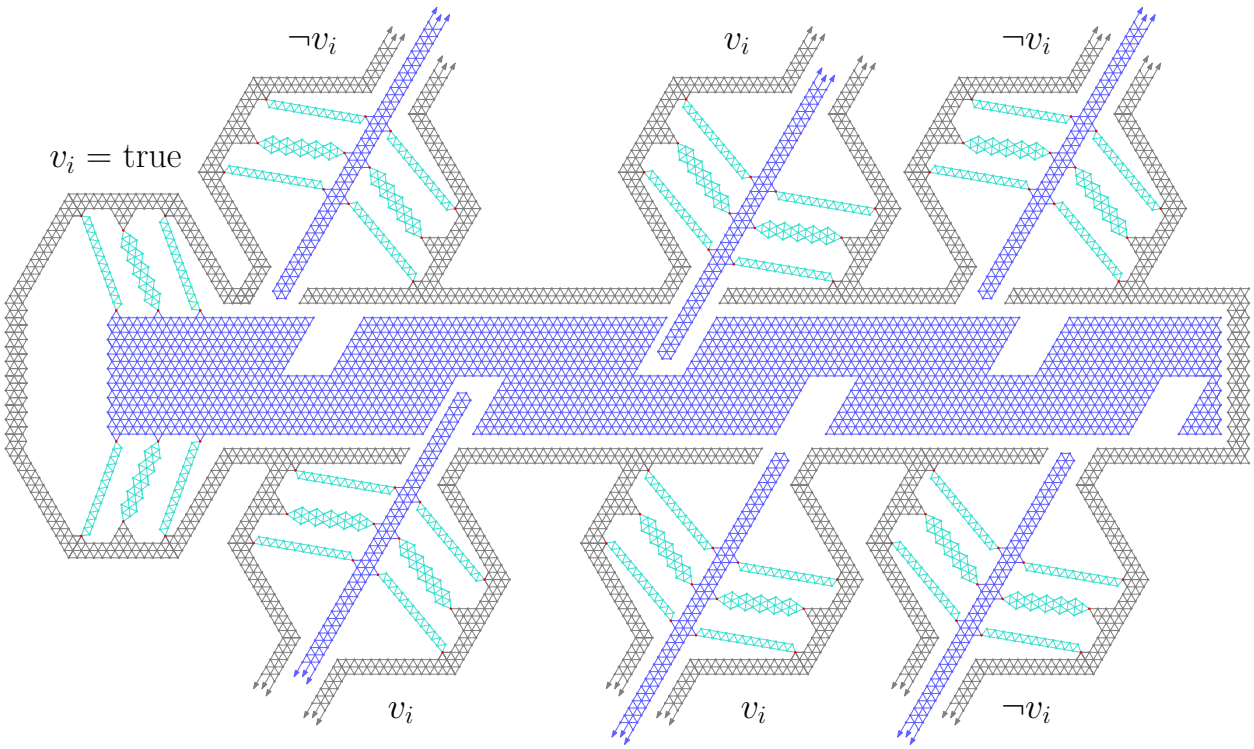

(a)

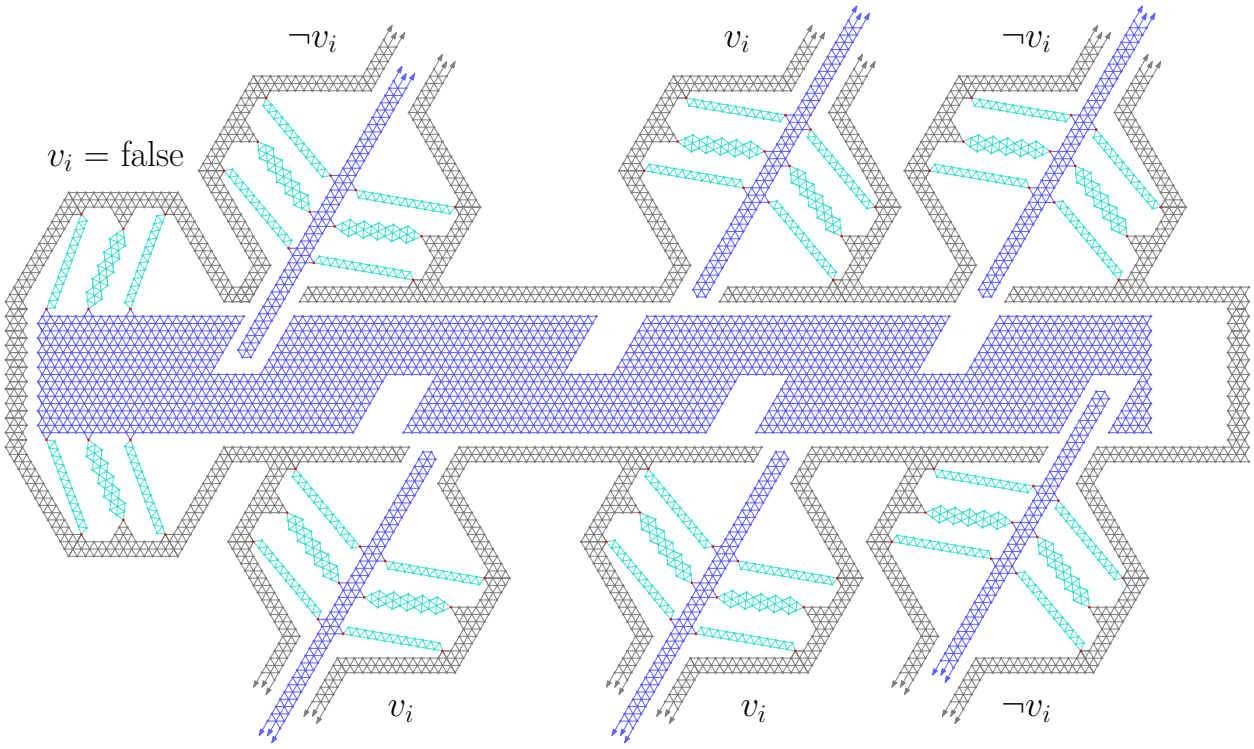

(b)

Figure 4.8: The Variable Gadget. (a) The 'true' configuration of the variable gadget. In this configuration, nonnegated literals' wires can be pushed in towards the gadget. (b) The 'false' configuration of the variable gadget. In this configuration, negated literals' wires can be pushed in towards the gadget.

Observe how the variable bar contain an indentation for each literal, so that in the 'true' configuration of the variable gadget in Figure 4.8a, the variable bar's indentations extend the length of the tunnel for non-negated literals, allowing their wire gadgets to be pushed toward the variable. Similarly, in the 'false' configuration of the variable gadget in Figure 4.8b, the variable bar's indentations elongate the tunnel for negated literals, so that they may be pushed towards the variable. Thus, we have that the wire gadgets transmit that a literal is 'true' through pressure towards the variable gadget, and that a literal is 'false' through pressure away from the variable gadget.

Our variable gadget mainly differs from that of [1] because it reuses structures of the holder gadget, which we have constructed differently for our problem. However, the other parts of the gadget are again triangular grid structures, which are allowed in both problems, so that the high-level structure of both variable gadgets is the same.

By Lemma A.4.1, we have that both of these configurations (with associated wire gadget actions) are realizable within the problem constraints. And by Corollary A.4.2 we have that forcing a false literal's wire (i.e. the wire of a non-negated literal in the 'false' variable gadget configuration or a negated variable in the 'true' variable gadget configuration) in towards the variable gadget (configuration not shown) is not possible within the problem constraints. However, as a consequence of Lemma A.4.1, we still have that a true literal's wire need not be pushed in towards the variable gadget (as seen with the botton center literal in Figure 4.8a and the top right literal in Figure 4.8b). Clearly, though, this behavior cannot mess up our construction, as it only allows us to decrease the number of 'true' literal values transmitted to our clause gadget.

We can now return to address the existence of the turn gadget configuration in Figure 4.7b. As we just established, pressure towards the variable is used to transmit a 'true' value. Thus, since the turn gadget configuration in question transmits pressure away from the turn for both of its associated wire gadgets, this configuration would have the effect of converting pressure towards the variable into pressure away from the variable; in other words, it would convert the transmitted 'true' value of a literal into a 'false' value. Thus, for the same reasons as before, this behavior cannot mess up our construction.

Now, we need to describe a clause gadget that is only realizable if it contains at least one wire with pressure away from the clause. However, it seems to be easier to design a clause gadget of the opposite nature, that is only realizable if it contains at least one wire with pressure towards the clause. To be able to do this, we introduce a new gadget, the inverter gadget, as shown in Figure 4.9. The inverter gadget allows us to convert pressure towards the variable into pressure away from the variable, and vice versa, as shown in Figures 4.9b and 4.9a. The thick green dots in the figure are used to show the possible positions of the ends of the left and right wires. Notice how we sandwich the inverter gadget between two holder gadgets to ensure the rigidity of the two wires extending from the gadget.

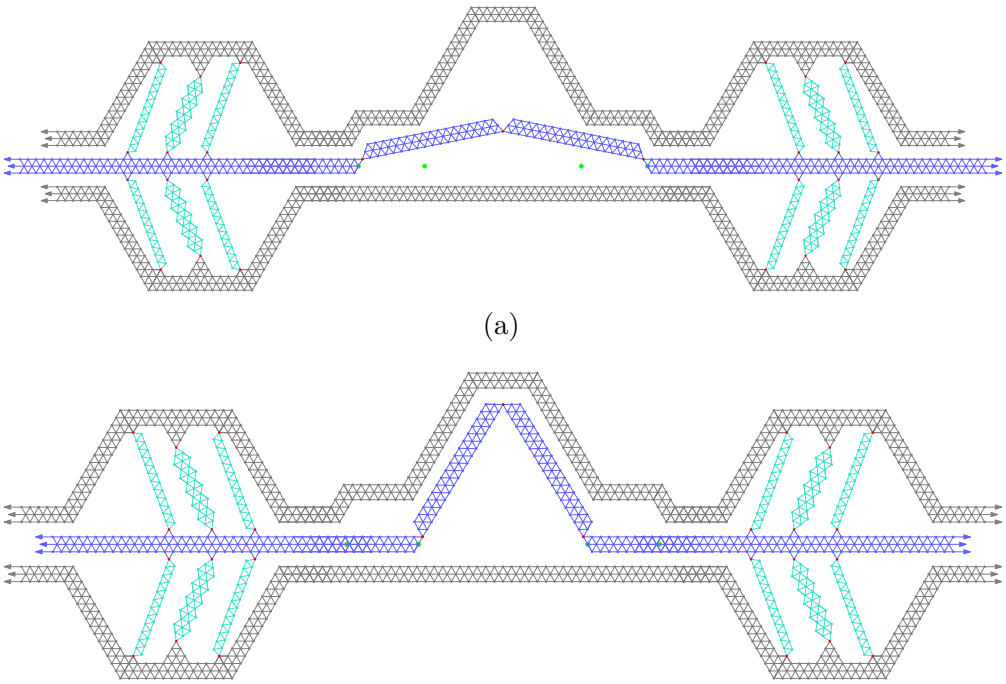

(a)

(b)

Figure 4.9: The Inverter Gadget (a) & (b) The two valid configurations of this gadget show how it inverts the pressure of a wire..

Our inverter gadget differs from that in [1] mainly due to the way the two constructions handle pivots within the respective problem constraints, as already seen with the holder gadget.

By Lemmas A.5.1, A.5.2, A.5.3 and A.5.4, we have that the two aforementioned desired configurations of the inverter gadget are realizable within the problem constraints. Also, by Lemma A.5.5, we have that the two unwanted configurations of the inverter gadget shown in Figure 4.10 (as well as their mirror images, since the gadget is symmetric), in which the pressure of the wires is not inverted, are not realizable within the problem constraints. Note that we position the inverter gadget right before the the wire enters the clause gadget (in particular, after all turns in the wire), so that the harmlessness of the turn gadget configuration in Figure 4.7b still holds.

Note that while this construction forces a particular embedding for the wire gadget relative to the tunnel gadget, each of the two central blue structures inside the gadget still has two possible planar embeddings. However, by an analogous argument to our discussion of the struts of the holder gadget, the inverter gadget cannot be subverted by use of an alternated embedding of one of these structures. As before, these only allow the possibility to do worse than our suggested embedding by possibly causing the gadget to fail to satisfy the problem constraints in the previously verified configurations in 4.9.

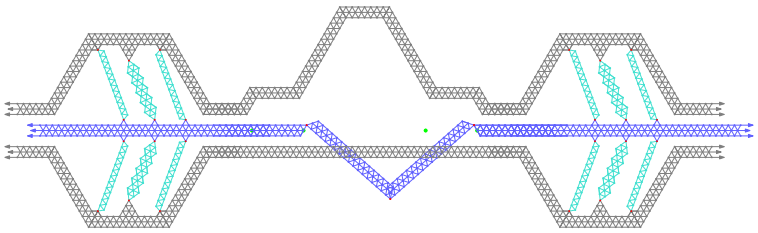

(a)

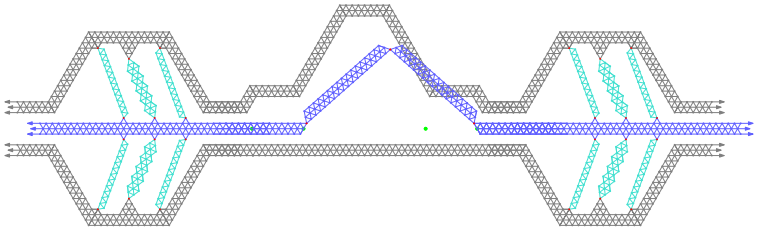

(b)

Figure 4.10: The Invalid Configurations of the Inverter Gadget. (a) & (b) show the two invalid configurations of the gadget.

Now, we can begin to discuss the clause gadget. As previously mentioned, we would like to design our clause gadget to be realizable only if it contains at least one wire with pressure towards the clause (which now means that it contains at least one 'true' literal). In fact, observe that it suffices to design our clause gadget to be realizable only if it contains exactly one 'true' literal, disregarding configurations with two or more 'true' literals.

This is because, as we saw when we first introduced the variable gadget, even if a variable assignment allows a particular literal to be true, the literal's wire can still transmit the value of that literal to be 'false'. Thus, whenever a particular clause has more than one literal that can evaluate to be 'true', we can have all but one of these literals transmit a 'false' value instead without changing the overall truth value of the clause, so that we only need to ensure the gadget functions correctly for clauses with 0 or 1 true literals.

Keeping this in mind, we can finally introduce our clause gadget, whose four configurations we care about are shown in Figure 4.8. The green dots show the position of the edge of the wire gadgets entering the clause gadget, for both the true and false values of each literal (the dot closer to the center corresponding to a 'true' literal). Each wire entering the gadget is connected to a rigid 'arm' structure that can pivot about the tip of the wire. The three arms are then joined at their tips in a triangle configuration.

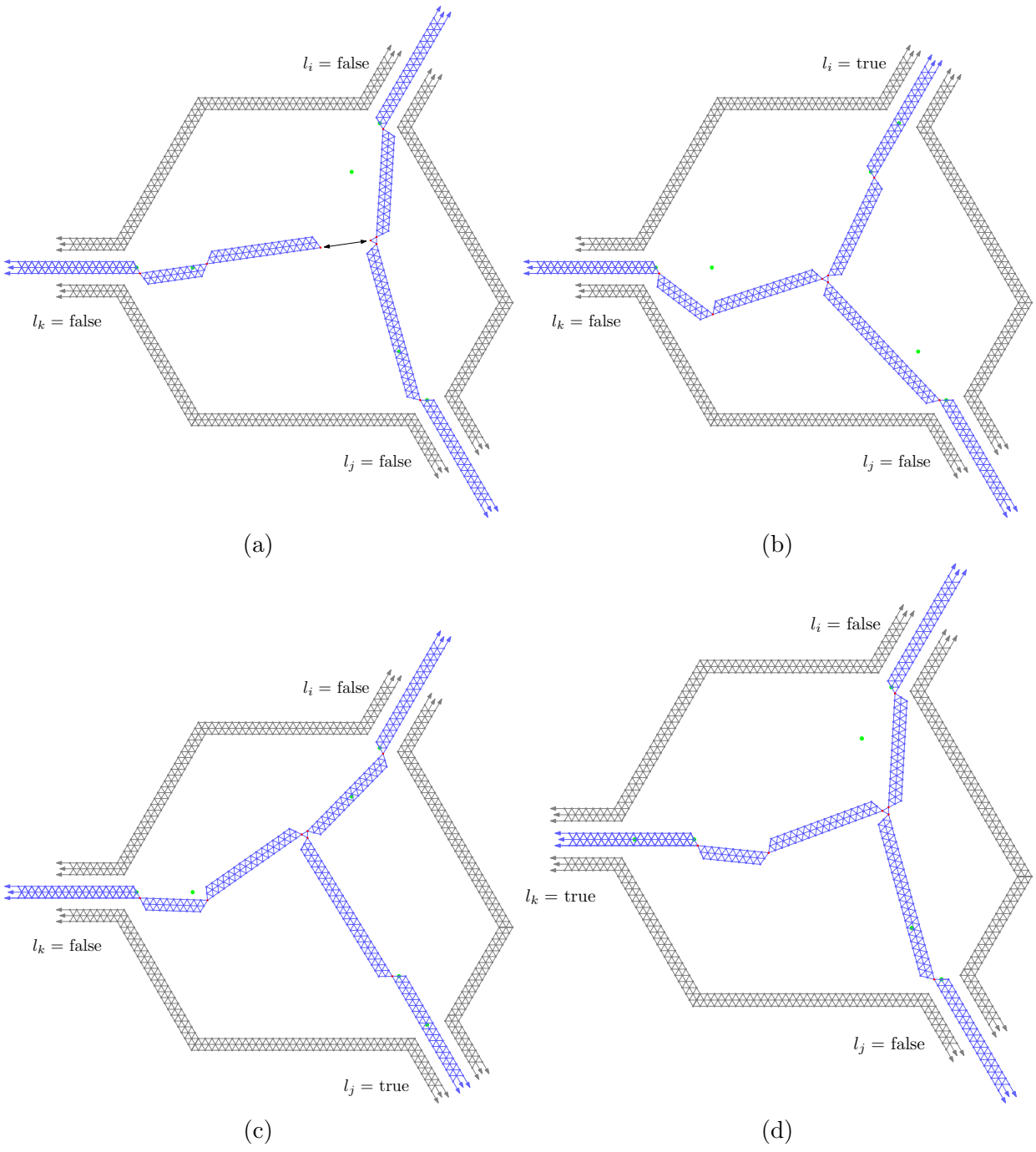

Figure 4.11: The Clause Gadget. (a) The unrealizable configuration of the clause gadget, with three 'false' literals. The pressure of all three incoming wires is away from the gadget. The arrows point to the two points which should coincide. (b), (c), and (d) The realizable configurations of the clause gadget, with one 'true' literal (for which the pressure of the corresponding wire is towards the gadget) and two 'false' literals (in which the pressure of the corresponding wires is away from the gadget).

Our clause gadget significantly differs from that in [1] because of the aforementioned handling of pivots within the respective problem constraints. It also differs from [1] in that we have the tips of our 'arm' structures connected in a triangle, rather than directly coinciding, due to the angle constraints of our problem. Lastly, our clause gadget differs from that in [1] because of our earlier observation about halving the number of cases our clause gadget needed to handle. Interestingly, while this observation is equally valid in the case of Cabello et al.'s proof, they did not choose to make use of it.

By Lemmas A.6.2, A.6.3, A.6.4, A.6.5, A.6.6, and A.6.7 we have that the three configurations of the clause gadget with one 'true' literal (shown in Figures 4.11b, 4.11c, and 4.11d) are realizable within the problem constraints. However, by Lemma A.6.1, we have that the configuration with all 'false' literals (shown in Figure 4.11a) is not realizable within the problem constraints. Thus, recalling our observation, our clause gadget correctly requires at least one 'true' literal to be realized.

Once again, note that while this construction forces a particular embedding for the wire gadgets relative to the tunnel gadgets, each part of the three blue 'arm' structures inside the gadget still has two possible planar embeddings. However, by an analogous argument to our discussion of the struts of the holder gadget, the clause gadget cannot be subverted by use of an alternated embedding of one of these structures. As before, these only allow the possibility to do worse than our suggested embedding by possibly causing the gadget to fail to satisfy the problem constraints in the previously verified configurations in 4.11b-d.

A small example with all of the gadgets working together is shown in Figure 4.12.

To summarize, our clause gadget is realizable if and only if exactly one literal transmitted a 'true' value, which means that the corresponding wire is pushing in towards the clause gadget. This implies that on the far side of the inverter gadget from the clause, the corresponding wire has pressure towards the variable. This pressure is propagated through the wires and turns until the variable gadget, where the wire is pushing in towards the variable gadget, which is only possible if the variable's truth value is that of the corresponding literal. Since our variable gadget allows true literal to transmit a 'false' value through the wire gadget, our construction also functions correctly for clauses containing more than one true literal. Thus, our entire constructed graph is only realizable (within the problem constraints) if all PR3SAT clauses are satisfied. Finally, our constructed graph has a polynomial number of edges since the graph of the original PR3SAT instance was in a grid of polynomial size, and thus, our reduction is in polynomial time. □

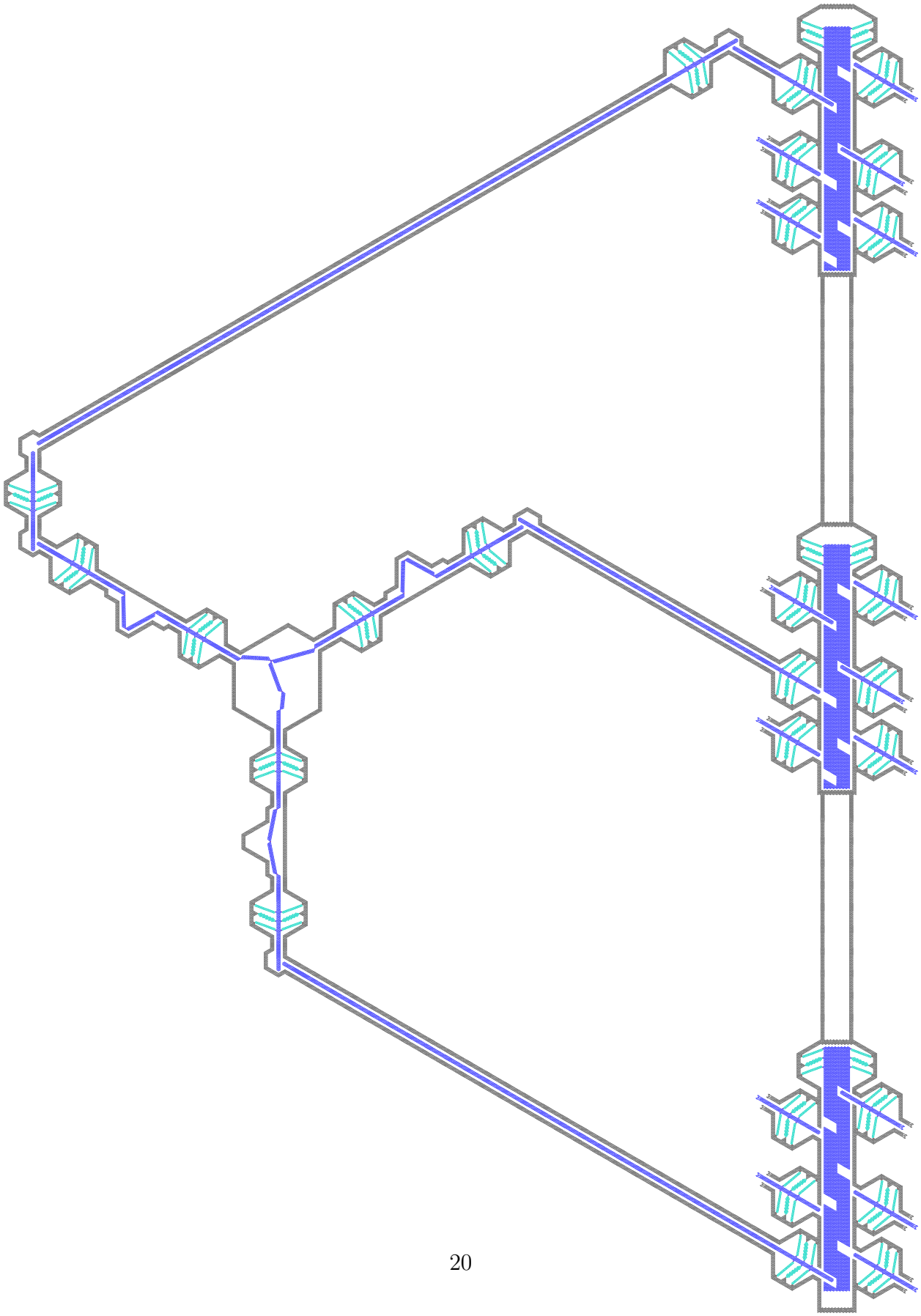

Figure 4.12: A small example of all gadgets working together.

Acknowledgements

I would like to thank Prof. David Jerison, Prof. Ankur Moitra, and Prof. Slava Gerovitch for organizing the UROP+ program and allowing me this research opportunity. I would also like to thank Vishal Patil for his mentoring. Finally, I would like to thank the Ralph L. Evans (1948) Endowment Fund, for generously funding this research. Most of all, I would like to thank my parents, for their support during this program.

References

[1] Sergio Cabello and E. Demaine and G. Rote, *Planar Embeddings of Graphs with Specified Edge Lengths*, Graph Drawing, 2003.

[2] Sebastian Morr and C. Scheffer, *Split Packing : An Algorithm for Packing Circles with up to Critical Density* (2016).

[3] David Lichtenstein, *Planar Formulae and Their Uses*, SIAM J. Comput. **11** (1982), 329-343, DOI 10.1137/0211025.

[4] Donald E. and Raghunathan Knuth Arvind, *The problem of compatible representatives*, SIAM Journal on Discrete Mathematics **5** (1992), no. 3, 422–427, DOI 10.1137/0405033.

[5] R. Fowler and M. Paterson and S. Tanimoto, *Optimal Packing and Covering in the Plane are NP-Complete*, Inf. Process. Lett. **12** (1981), 133-137.

[6] Erik D. Demaine and Sándor P. Fekete and Robert J. Lang, *Circle Packing for Origami Design Is Hard*, ArXiv **abs/1008.1224** (2010).

[7] H. Alt and K. Buchin and Steven Chaplick and O. Cheong and P. Kindermann and C. Knauer and Fabian Stehn, *Placing your Coins on a Shelf*, JoCG **9** (2018), 312-327.

[8] Heinz Breu and David G. Kirkpatrick, *Unit disk graph recognition is NP-hard*, Comput. Geom. **9** (1998), 3-24.

[9] Matthew William Brems and Alexander Wagner, *Equal Circle Packing on a Square Flat Klein Bottle* (2012).

[10] André and Schneider Müller Johannes and Schömer, *Packing a multidisperse system of hard disks in a circular environment*, Physical review. E, Statistical, nonlinear, and soft matter physics **79** (2009), 021102, DOI 10.1103/PhysRevE.79.021102.

[11] Andrew Przeworski, *Packing Disks on a Torus*, Discrete & Computational Geometry **35** (2006), 159-174.

A Appendix A: Analyzing the Gadgets

In this appendix, we will use analytic geometry techniques to show that each of the gadgets used in our above reduction obey the constraints of disk packing, i.e. the circle geometry constraints mentioned in Section 1. Recall that our problem deals with disks of unit diameter, so that if two disks are touching, then the vertices corresponding to their centers in the contact graph are exactly 1 unit apart. Thus, we will show, for each of the gadgets, that if two vertices are not connected by an edge in the contact graph of the gadget, then they are greater than 1 unit apart. Again, because of the nature of circle geometry, we will also show that all angles between nonadjacent vertices with a common neighboring vertex are greater than 60°. Note that we will be using degrees to measure all of our angles, for a more intuitive understanding of non-standard angles, and that we will often give approximations to the nearest thousandth, for a more intuitive understanding of complicated measurements.

A.1 The Basics

In this section, we examine some of the basic properties used in the remainder of this appendix, ending with a short proof of the realizability of the tunnel/wire gadget within the problem constraints.

For most of the following analyses, we will begin by overlaying the gadgets onto a triangular grid. As we will often use this grid to help measure distances between lattice points, we begin by noting a few of its properties we will use (note: throughout this appendix, we will refer to both grids and lattices, using grids to refer to the infinite repeating collection of lines and lattices refer to the infinite repeating collections of points; there is a clear correspondence between the two).

All of the gadgets consist of several components, where each component is a rigid subset of a triangular grid/lattice (edges/vertices), though each component may be a part of a different grid/lattice. However, note that the outer rigid parts of the tunnels and other gadgets all share the same lattice/grid, which we refer to as the "tunnel lattice"/"tunnel grid" (this is basically all of the parts of the gadgets that are colored gray).

We now review properties of the triangular lattice which are useful in measuring distances in our proof, shown in Figure A.1a (note that because the triangular grid has rotational symmetry, these properties also apply in different orientations). Taking the lattice vectors to be unit length (which corresponds to disks in the contact graph having diameter 1), we have that the horizontal distance between a lattice point and its horizontally adjacent lattice point is 1 (i.e. the distance from A to B is 1). Furthermore, we have the vertical distance between adjacent rows of lattice points is $\frac{\sqrt{3}}{2}$ (i.e. the distance between $\overleftrightarrow{AB}$ and $\overleftrightarrow{CD}$ is $\frac{\sqrt{3}}{2}$). Finally, note that the horizontal displacement between adjacent lattice points in different

rows is $\frac{1}{2}$ (i.e. the horizontal displacement between A and C is $\frac{1}{2}$).

Finally, we end by verifying that the tunnel/wire gadget can be verified within the problem constraints

Lemma A.1.1. *The tunnel and wire gadgets are greater than unit distance apart.*

Proof. In the tunnel gadget (see Figure A.1b), while the wire gadget's lattice/grid (which we call the "wire lattice"/"wire grid" is shifted horizontally from the "tunnel lattice"/"tunnel grid", it is not at all shifted vertically from the "tunnel lattice"/"tunnel grid", so that by construction, we have that the distance from the wire gadget to the sides of the tunnel gadget is $\sqrt{3} > 1$. □

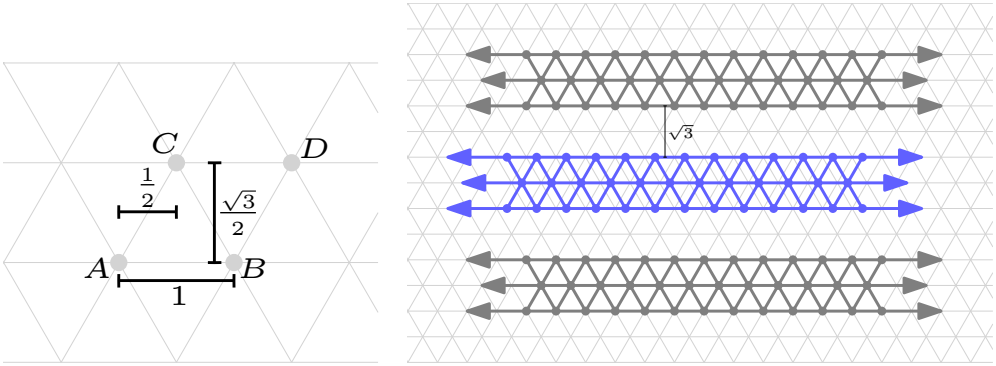

(a) (b)

Figure A.1: (a) Triangular grid properties (b) The Tunnel Gadget

A.2 The Holder Gadget

UPDATE FIGURES!!!! THIS SECTION IS NOT COMPLETE!!!

First, we examine the holder gadget (see Figure A.2), and prove that its two valid configurations are realizable within the constraints of the problem. We also quantify the shift of the wire grid with respect to the tunnel grid. Note that in this analysis, we refer to the turquoise structures of the holder gadget as "struts".

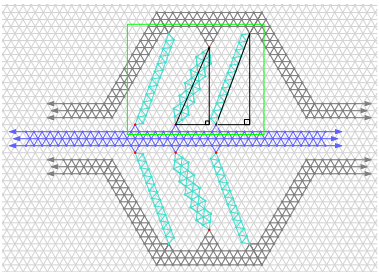

(a)

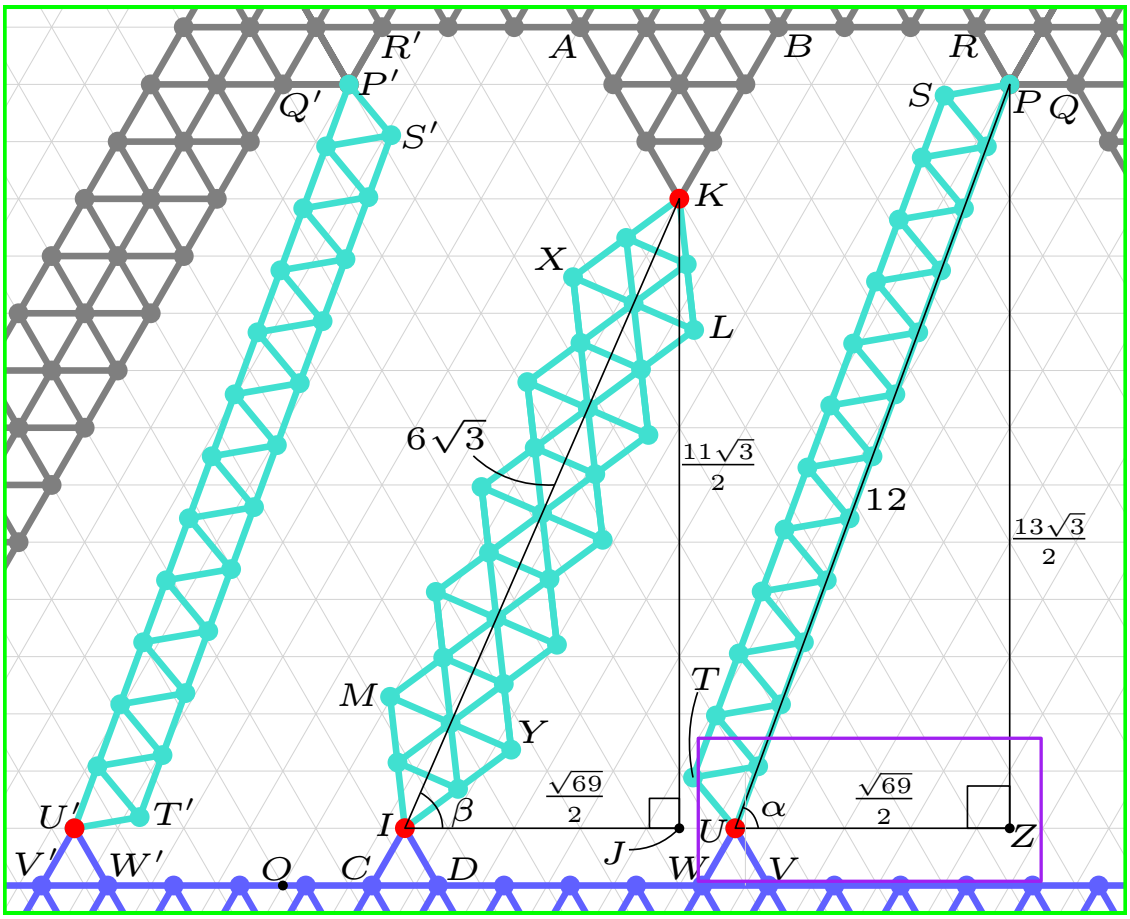

(b)

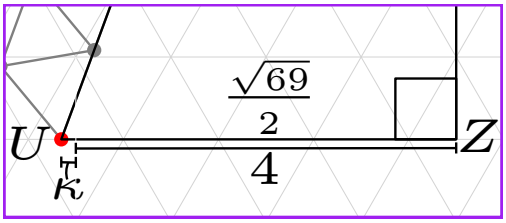

(c)

Figure A.2: The Holder Gadget. (a) The Holder Gadget overlaid on the triangular grid of the tunnel. (b) Close-up of the top right strut. (c) Close-up of the top left strut. (d) Close-up of the shift.

Lemma A.2.1. *The angles between adjacent components of the holder gadget are all greater than* $60°$.

Proof. We begin by overlaying the gadget onto the triangular grid of the sides of the tunnel (the "tunnel grid"), like in Figure A.2a. Now, we can focus our analysis on just the top half of one of the realizations of the holder gadget as shown in Figure A.2b (a close-up of the region outlined in green in A.2a), since the bottom half and the other realization consist of just rotated and reflected versions of this gadget, which doesn't change angles or distances.

Let us start by focusing on the right strut. By construction, we know that $UP = 12$ and that $ZP = \frac{13\sqrt{3}}{2}$. Thus, since $\angle UZP$ is a right angle we have that $m\angle ZUP = \alpha = \sin^{-1}(\frac{13\sqrt{3}}{24}) \approx 69.750°$. Also, note by the Pythagorean Theorem that $ZU = \frac{\sqrt{69}}{2}$.

Since $m\angle ZPQ = 90°$, we have that $m\angle UPQ = 90° - \alpha + 90° = 180° - \alpha \approx 110.250°$, so that $m\angle UPQ > 60°$. Because $m\angle RPQ = 120°$ and $m\angle SPU = 60°$, we have that $m\angle RPS = 180 - m\angle UPQ = \alpha \approx 69.750°$, so that $m\angle RPS > 60°$.

Next, we have that $m\angle ZUV = 60°$, so that $m\angle VUP = 60° + \alpha \approx 129.750°$, so that $m\angle VUP > 60°$. Because $m\angle TUP = 60°$ and $m\angle WUV = 60°$, we have that $m\angle TUW = 240° - m\angle VUP = 180° - \alpha \approx 110.250°$, so that $m\angle TUW > 60°$

Let us now move our analysis to the left strut. Recall that $\overline{U'P'} \parallel \overline{UP}$.

Since $\overline{U'P'}$ makes an angle of $90° - \alpha$ with the vertical at P', we have that $m\angle U'P'Q' = \alpha \approx 69.750°$, so that $m\angle U'P'Q' > 60°$. Because $m\angle U'P'S' = 60°$ and $m\angle Q'P'R' = 120°$, we have that $m\angle R'P'S' = 180 - m\angle U'P'Q' = 180° - \alpha \approx 110.250°$, so that $m\angle R'P'S' > 60°$.

Then, by adjacent interior angles, we have that $m\angle P'U'V' = 60° + (180° - m\angle U'P'Q') = 240° - \alpha \approx 170.250°$, so that $m\angle P'T'V' > 60°$. Because $m\angle V'U'W' = 60°$ and $m\angle P'U'T' = 60°$, we have that $m\angle T'U'W' = 240° - m\angle P'T'V' = \alpha \approx 69.250°$, so that $m\angle T'U'W' > 60°$.

Now, we shift our analysis to the middle strut. By construction, we have that $IK = 6\sqrt{3}$ and that $KJ = \frac{11\sqrt{3}}{2}$. Thus, since $\angle IJK$ is a right angle we have $m\angle KIJ = \sin^{-1}\left(\frac{\frac{11\sqrt{3}}{2}}{6\sqrt{3}}\right)$. Let $m\angle KIJ = \beta$. Also note, by the Pythagorean Theorem, that $IJ = \frac{\sqrt{69}}{2}$.

Since $m\angle DIJ = m\angle MIY = 60°$, and $\overline{IK}$ bisects $\angle MIY$, We know that $m\angle YIJ = m\angle KIJ - 30°$, so that $m\angle YID = \beta + 30° \approx 96.444°$, so that $m\angle YID > 60°$. Since $m\angle MIY = m\angle CID = 60°$, we have that $m\angle MIC = 240° - m\angle YID = 210° - \beta \approx 143.556°$, so that $m\angle MIC > 60°$.

Now, since $\overleftrightarrow{ID} \parallel \overleftrightarrow{AK}$ and $\overleftrightarrow{IY} \parallel \overleftrightarrow{XK}$, we have that $m\angle AKX = m\angle YID = \beta + 30° \approx 96.444°$, so that $m\angle AKX > 60°$. Also, since $m\angle AKB = m\angle XKL = 60°$, we have that $m\angle BKL =$

$240° - m\angle AKX = 210° - \beta \approx 143.556°$, so that $m\angle BKL > 60°$. □

Corollary A.2.2. *The wire gadget is shifted by $\sqrt{69}$ units (in the direction parallel to the wire) between the two configurations of the holder gadget.*

Proof. As determined in the previous proof, $IJ = UZ = \frac{\sqrt{69}}{2}$ is the shift of the wire gadget from being "centered" on our holder gadget. Since the other configuration of the holder gadget (Figure 4.3b is a mirror image of the configuration shown in Figure 4.3a, we have that the distance (shift) between the two configurations of the wire gadget is $\frac{\sqrt{69}}{2} \cdot 2 = \sqrt{69}$. □

Next, let us examine the shift of triangular lattice of the the wire gadget (the "wire lattice") with respect to the "tunnel lattice"(The triangular lattice of the tunnel gadget), by examining Figure A.2c (a close-up of the region outlined in green in A.2b. Recall that $UZ = IJ = \frac{\sqrt{69}}{2}$. We define the following constant to simplify later calculations using this shift.

Definition A.2.3. Let $\kappa = \frac{\sqrt{69}}{2} - 4 \approx 0.153$.

We now quantify the shift.

Lemma A.2.4. *The "wire grid" is shifted by $\kappa + \frac{1}{2}$ from the "tunnel grid" in the direction of pressure.*

Proof. Noting that Z is at the midpoint between two lattice points of the "tunnel lattice", we find that the "wire lattice" is shifted by $\kappa + \frac{1}{2}$ in the direction of "pressure" from the "tunnel lattice". Note that this means that while no points coincide between the two lattices, we have that all lines of the "tunnel grid" are parallel to or the same as the corresponding [shifted] lines of the "wire grid" (the triangular grid of the "wire lattice"). □

Note that while we may reuse and/or redefine other symbols and/or variables in the analysis of different gadgets, we use this same value of κ throughout this appendix.

Finally, we complete the verification of the holder gadget.

Lemma A.2.5. *The disjoint components of the holder gadget are greater than unit distance apart.*

Proof. Because we have already verified all relevant angles, it only remains to show that adjacent struts are greater than unit distance apart. Again, refer to Figure A.2b.

First, for the right and middle struts, we want to calculate the distance between their closest edges. Because $m\angle KIJ = \beta$ and $m\angle PUZ = \alpha$, and since $\tan\beta < \tan(\beta)$, we have that the slope of $\overleftrightarrow{IK}$ is less than the slope of $\overleftrightarrow{UP}$. Since $\overleftrightarrow{YL} \parallel \overleftrightarrow{KI}$ and $\overleftrightarrow{TS} \parallel \overleftrightarrow{UP}$, due to their slopes

and relative positions, it suffices to check that L is more than unit distance from $\overline{TS}$ to verify that the two struts are far enough apart.

Similarly, for the left and middle struts, we also want to calculate the distance between their closest edges. Since $\overleftrightarrow{MX} \parallel \overleftrightarrow{KI}$ and $\overleftrightarrow{T'S'} \parallel \overleftrightarrow{UP}$, due to their slopes and relative positions, it suffices to check that M is more than unit distance from $\overline{T'S'}$ to verify that the two struts are far enough apart.

To accomplish this, we will calculate the positions of points in a Cartesian coordinate system. By fixing the origin $(0, 0)$ to O (note that O is a point in the "tunnel lattice"), we can calculate the Cartesian coordinates of other points from their horizontal and vertical displacement from O using the triangular grid, our shift calculations from A.2.4, and trigonometry.

First, by construction, we find that $I = (2 - \kappa, \frac{\sqrt{3}}{2})$, $U = (7 - \kappa, \frac{\sqrt{3}}{2})$, and $U' = (-3 - \kappa, \frac{\sqrt{3}}{2})$. Next, since $m\angle YIJ = \beta - 30°$, $m\angle MIJ = \beta + 30°$, and $MI = YI = 2$, we have that $Y = (2 - \kappa + 2\cos(\beta - 30°), \frac{\sqrt{3}}{2} + 2\sin(\beta - 30°))$, and that $M = (2 - \kappa + 2\cos(\beta + 30°), \frac{\sqrt{3}}{2} + 2\sin(\beta + 30°))$. Additionally, since $m\angle KIJ = \beta$, $\overleftrightarrow{KI} \parallel \overleftrightarrow{LY}$, and $LY = 4\sqrt{3}$, we have that $L = (2 - \kappa + 2\cos(\beta - 30°) + 4\sqrt{3}\cos\beta, \frac{\sqrt{3}}{2} + 2\sin(\beta - 30°) + 4\sqrt{3}\sin\beta)$. Also, since $m\angle TUZ = \alpha + 60°$, $m\angle T'U'I = \alpha - 60°$, and $TU = T'U' = 1$, we have that $T = (7 - \kappa + \cos(\alpha + 60°), \frac{\sqrt{3}}{2} + \sin(\alpha + 60°))$ and $T' = (-3 - \kappa + \cos(\alpha - 60°), \frac{\sqrt{3}}{2} + \sin(\alpha - 60°))$.

Now, using the fact that the slope of $\overleftrightarrow{TS}$ = the slope of $\overleftrightarrow{T'S'} = \tan\alpha$, we can find the equations of these lines. Then, using the equation for the distance from a point to a line (given a line in standard form $ax + by + c = 0$ and a point (x_0, y_0), the distance from the point to the line is $\frac{|ax_0+by_0+c|}{\sqrt{a^2+b^2}}$). We find that the distance between $\overleftrightarrow{TS}$ and L is $\frac{235\sqrt{3}}{144} - \frac{5\sqrt{23}}{48} \approx 2.327$, so that L is greater than unit distance from $\overline{TS}$, and that the distance between $\overleftrightarrow{T'S'}$ and M is $\frac{\sqrt{23}}{48} + \frac{235\sqrt{3}}{144} \approx 2.927$, so that M is greater than unit distance from $T'S'$. □

A.3 The Turn Gadget

Now, we examine the turn gadget (see Figure A.3).

Lemma A.3.1. *The disjoint components of the turn gadget are greater than unit distance apart.*

Proof. As before, we begin by overlaying the gadget onto the "tunnel lattice", like in Figure A.3a. We only focus our analysis on only one of the realizations of the holder gadget, since the two are mirror images of each other.

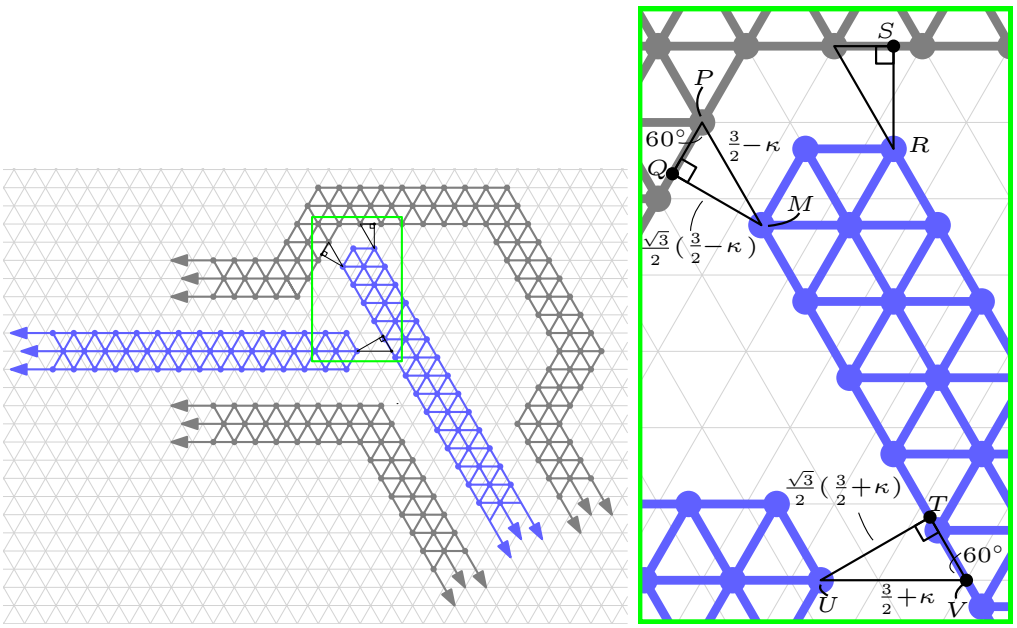

(a) (b)

Figure A.3: The Turn Gadget. (a) The Turn Gadget overlaid on the triangular grid of the tunnel. (b) Close-up of the relevant gaps.

Let us begin by calculating the distance between the two wires of the gadget, as shown in the bottom of Figure A.3b (a close-up of the region outlined in green in A.3a). Note that we are dealing with two separate "wire grid"s here (left and right), because each wire is shifted in a different direction with respect to the "tunnel grid". However, since corresponding lines in the shifted "wire grid"s are parallel to the lines in the "tunnel grid", they are also parallel to each other. Thus, to show that the two wires are sufficiently far apart, it suffices to show that U (of the left wire) is greater than unit distance from T, the closest point to U on $\overleftrightarrow{TV}$ (of the right wire). Note that $\overleftrightarrow{TV}$ belongs to both the "tunnel grid" and the right "wire grid", and that V belongs to the "tunnel lattice".

Recalling our previous shift calculations form Lemma A.2.4, we find that $UV = \frac{3}{2} + \kappa$, by construction. Furthermore, since $\overleftrightarrow{UV}$ and $\overleftrightarrow{TV}$ are both parallel to lines of the "tunnel grid", we have that $m\angle UVT = 60°$. Thus, by right triangle trigonometry, we have that $UT = \frac{\sqrt{3}}{2}(\frac{3}{2} + \kappa) \approx 1.432$, so that $UT > 1$.

Now, we turn our attention to the distance between the end of the right wire and the wall of the gadget, as in the top of Figure A.3b. Again, since we have that the lines of the "wire grid" are parallel to the lines of the "tunnel grid", it suffices to check that M is greater than unit distance from Q (the closes point to M of $\overleftrightarrow{QP}$), and similarly that R is greater than unit distance from S. However, due to symmetry, we can check that $MQ = RS$, so that it

suffices to merely check the distance from M to Q.

Analogously, we find that $MP = \frac{3}{2} - \kappa$, by construction. Similarly, we again use that the "wire grid" and "tunnel grid" have parallel corresponding lines, so that $m\angle QPM = 60°$. Thus, by right triangle trigonometry, we have that $QM = \frac{\sqrt{3}}{2}(\frac{3}{2} - \kappa) \approx 1.166$, so that $QM > 1$. □

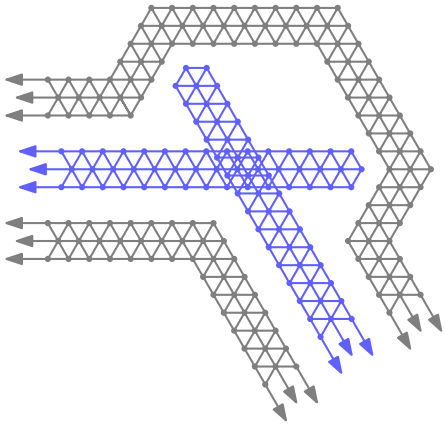

Figure A.4: The Invalid Configuration of the Turn Gadget

Lemma A.3.2. *The invalid configuration of the turn gadget cannot be realized within the problem constraints.*

Proof. From Lemma A.3.1, we have that the distance from the left wire to the right wire in Figure A.3b is $UV = \frac{3}{2} + \kappa$. By Corollary A.2.2, we have that the wire gadget is shifted by $\sqrt{69}$ units between the two configurations of the holder gadget. We know that $\sqrt{69} \approx 8.307$ and $\frac{3}{2} + \kappa \approx 1.653$, so that $\sqrt{69} > \frac{3}{2} + \kappa$. Thus, since we have that the left wire gadget is shifted $\sqrt{69}$ units to the right in the invalid configuration as compared to the configuration in Figure A.3b, the two wires must intersect in this configuration, so that it is invalid within the problem constraints. □

A.4 The Variable Gadget

Now, we examine the variable gadget (see Figure A.5, Figure A.7).

Note that this gadget includes multiple copies of the holder gadget, which we have already verified in A.2, so that we need not verify angles between adjacent structures of the variable gadget. Also note that the spacing between the variable bar and the outer wall of the gadget is the same as the tunnel gadget we verified in A.1. Thus, it only remains to verify the gaps between the variable bar and the ends of the wire gadgets. The gap calculation arguments in this section closely follow those of $A.3$.

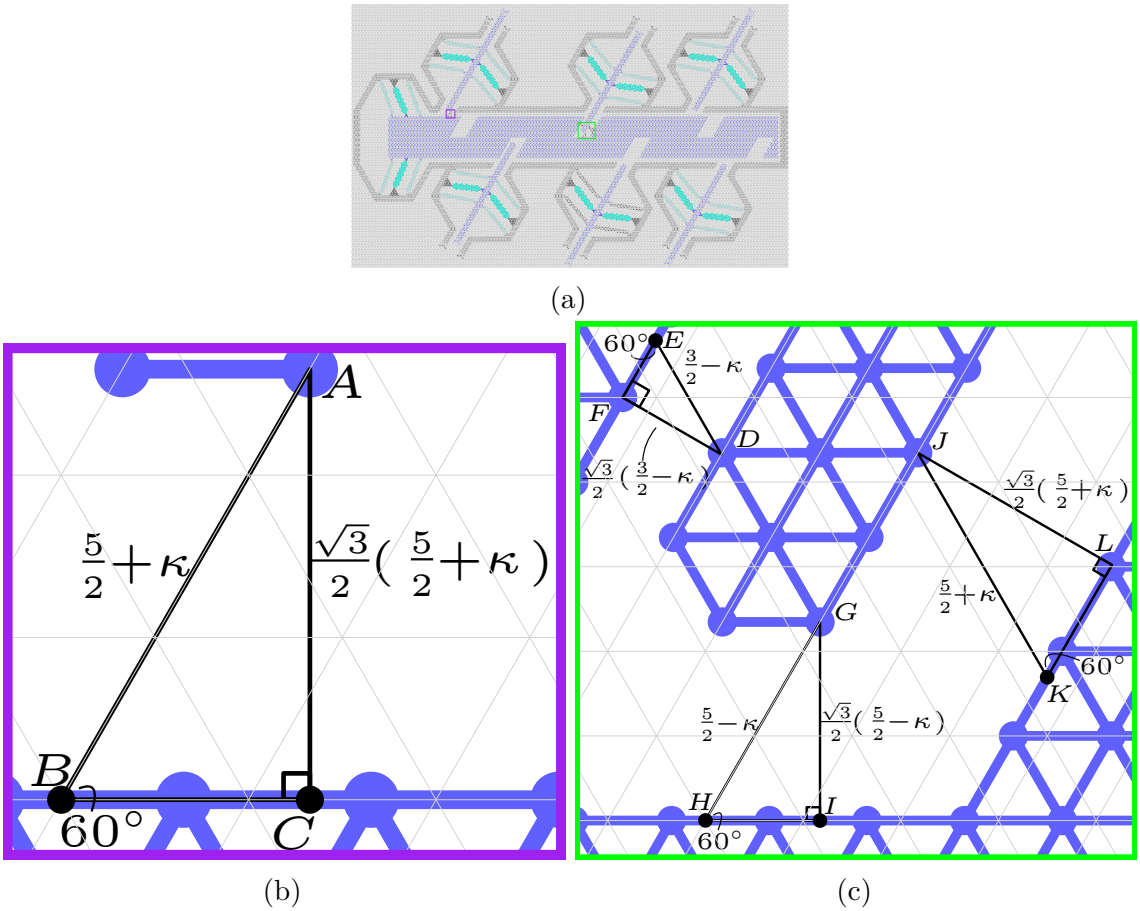

Figure A.5: The 'True' Variable Gadget. (a) The Variable Gadget overlaid on the triangular grid of the tunnel. (b) Close-up of the gap between the variable bar and a false literal. (c) Close-up of the gap between the variable bar and a true literal

Lemma A.4.1. *The disjoint components of the variable gadget are greater than unit distance apart.*

Proof. Let us begin by analyzing the 'true' configuration of the gadget. As before, we begin by overlaying the gadget onto the "tunnel lattice", like in Figure A.5a.

Let us begin by calculating the distance between the variable bar and the end of the wire gadget of a 'false' literal, as in Figure A.5b (a close-up view of the region outlined in purple in A.5a). Because the two "wire grids" are only shifted, not rotated, we have that corresponding lines are parallel, so that it suffices to show that A is a sufficient distance from C. Note that this distance will be the same for both the 'true' and 'false' configurations of this gadget, so we only need to verify it once.

As before, we find that $AB = \frac{5}{2} + \kappa$, by construction. Furthermore, since $\overleftrightarrow{AB}$ and $\overleftrightarrow{BC}$ are

both parallel to lines of the "tunnel grid", we have that $m\angle ABC = 60°$. Thus, by right triangle trigonometry, we have that $AC = \frac{\sqrt{3}}{2}(\frac{5}{2} + \kappa) \approx 2.298$, so that $AC > 1$.

Now, we turn our attention to the distance between the variable bar and a 'true' literal that is extended into its gap, as in Figure A.5c (a close-up view of the region outlined in green in A.5a). Again, since we have that the lines of the "wire grid" are parallel to the lines of the "tunnel grid", it suffices to check that D is greater than unit distance from F, G is more than unit distance from I, and J is more than unit distance from L.

Analogously to the the previous calculation, we find that $DE = \frac{3}{2} - \kappa$, $GH = \frac{5}{2} - \kappa$, and $JK = \frac{5}{2} + \kappa$, by construction. We also find that $m\angle DEF = m\angle GHI = m\angle JKL = 60°$. Thus, we find that $DF = \frac{\sqrt{3}}{2}\left(\frac{3}{2} - \kappa\right) \approx 1.166$, $GI = \frac{\sqrt{3}}{2}\left(\frac{5}{2} - \kappa\right) \approx 2.032$, and $JL = \frac{\sqrt{3}}{2}\left(\frac{5}{2} + \kappa\right) \approx 2.298$, so that $DF > 1$, $GI > 1$, and $JL > 1$.

Next, we analyze the 'false' configuration of this gadget (see Figure A.7), by again overlaying it onto the "tunnel lattice", as in Figure A.6a. As established above, we can immediately turn our attention to the distance between the variable bar and a 'true' literal that is extended into its gap, as in Figure A.6b (a close-up view of the region outlined in maroon in Figure A.6a).

Again, since we have that the lines of the "wire grid" are parallel to the lines of the "tunnel grid", it suffices to check that D' is greater than unit distance from F', G' is more than unit distance from I', and J' is more than unit distance from L'.

Almost exactly as before, we find that $D'E' = \frac{3}{2} + \kappa$, $G'H' = \frac{5}{2} - \kappa$, and $J'K' = \frac{5}{2} - \kappa$, by construction. We also find that $m\angle D'E'F' = m\angle G'H'I' = m\angle J'K'L' = 60°$. Thus, we find that $D'F' = \frac{\sqrt{3}}{2}\left(\frac{3}{2} + \kappa\right) \approx 1.432$, $G''I = \frac{\sqrt{3}}{2}\left(\frac{5}{2} - \kappa\right) \approx 2.032$, and $J'L' = \frac{\sqrt{3}}{2}\left(\frac{5}{2} - \kappa\right) \approx 2.032$, so that $D'F' > 1$, $GI' > 1$, and $J'L' > 1$. □

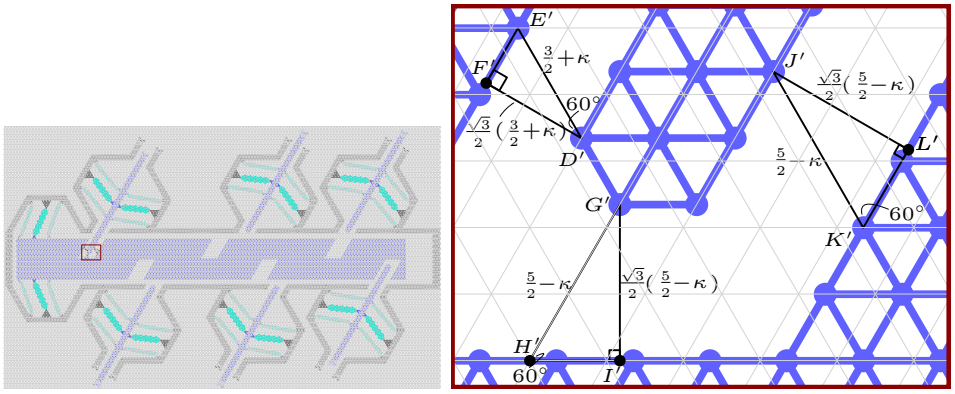

(a) (b)

Figure A.6: The 'False' Variable Gadget. (a) The Variable Gadget overlaid on the triangular grid of the tunnel. (b) Close-up of the gap between the variable bar and a true literal

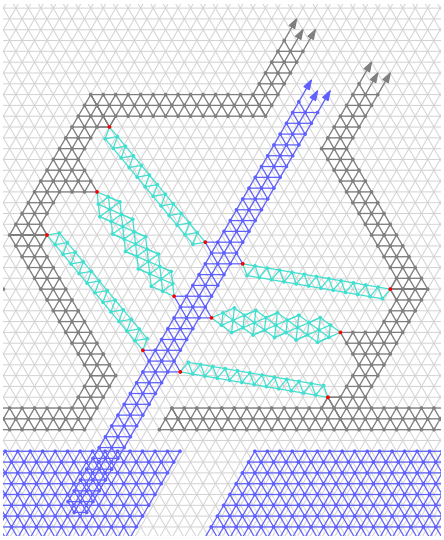

Figure A.7: An Invalid Forced Literal in the Variable Gadget

Corollary A.4.2. *It is impossible to force the wire gadgets of false literals (negated literals in the 'true' variable configuration or nonnegated literals in the 'false' variable configuration) towards the variable gadget.*

Proof. From Lemma A.4.1, we have that the distance from the end of the wire gadgets to the variable bar in Figure A.5b is $\frac{5}{2} + \kappa$ units when measured in the direction parallel to the wire. By Corollary A.2.2, we have that the wire gadget is shifted by $\sqrt{69}$ units between the two configurations of the holder gadget. We know that $\sqrt{69} \approx 8.307$ and $\frac{5}{2} + \kappa \approx 2.653$, so that $\sqrt{69} > \frac{5}{2} + \kappa$. Thus, since we have that the end of the wire gadget is shifted $\sqrt{69}$ units towards the variable gadget in the invalid configuration as compared to the configuration in Figure A.5b, the wire and variable bar must intersect in this configuration, so that it is invalid within the problem constraints. □

A.5 The Inverter Gadget

Our analysis of this gadget will be split into three parts, one to verify each of the two valid configurations of this gadget (the "outward" configuration, in which the "pressure" of the wire is directed away from the gadget on both sides, and the "inward" configuration, in which the "pressure" of the wire is directed towards the gadget from both sides) and one to prove the invalid configurations of the gadget.

A.5.1 The "Outward" Configuration

We first examine the "outward" configuration of the inverter gadget (see Figure A.8). We will first check angles before checking distances between the walls and inner structures of the gadget.

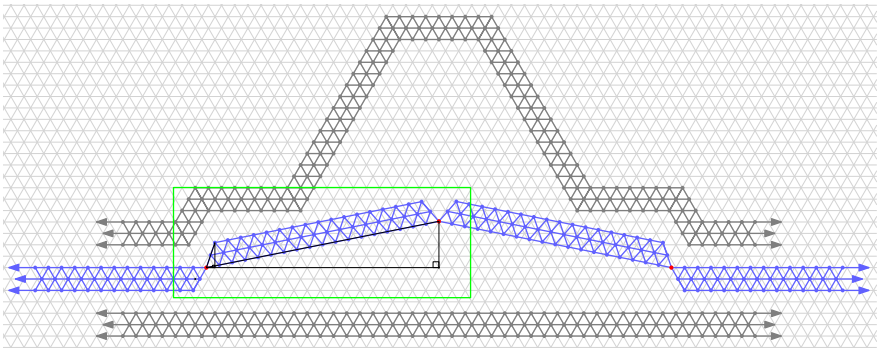

(a)

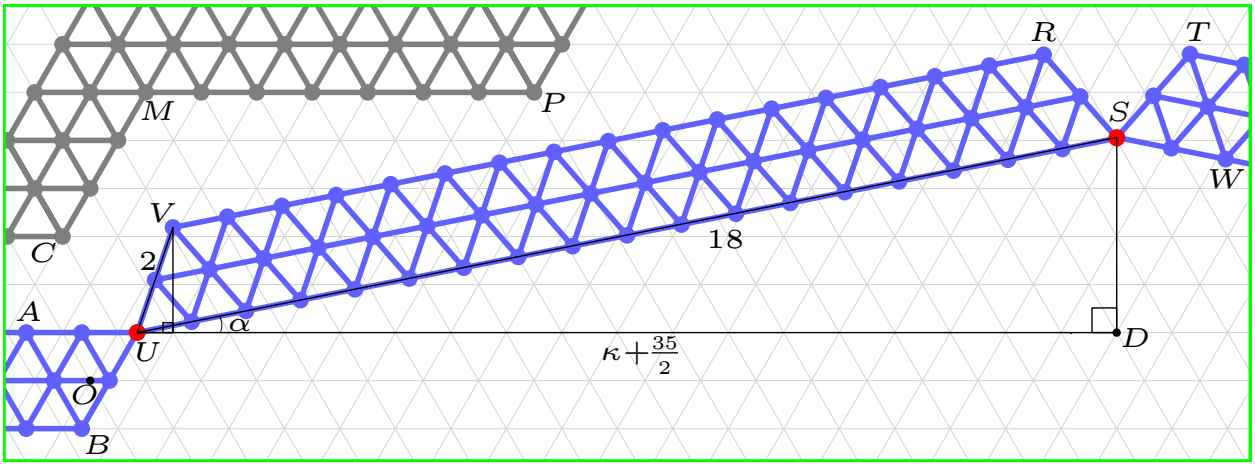

(b)

Figure A.8: The "Outward" Inverter Gadget. (a) The "Outward" Inverter Gadget overlaid on the triangular grid of the tunnel. (b) Close-up of the relevant parts of the gadget.

Lemma A.5.1. *The angles between adjacent components of the "outward" inverter gadget are all greater than* 60°.

Proof. As before, we begin by overlaying the gadget on top of the "tunnel lattice", like in Figure A.8a. We only focus our analysis on the left side of the gadget since the right side is a mirror image of the left side. Refer to Figure A.8b (a close-up of the region outlined in green in A.8a) for the following.

We begin by calculating $\alpha = m\angle SUD$. By construction, we have that $UD = \kappa + \frac{35}{2}$ and that

$US = 18$ (note that $\overleftrightarrow{DS}$ splits the gadget in half). Thus, $\alpha = \cos^{-1}(\frac{\kappa+\frac{35}{2}}{18}) \approx 11.263°$.

Since the left wire's "wire grid" is only horizontally shifted from the tunnel grid, we have that $m\angle BUD = 120°$. It follows that $m\angle SUB = 120° + \alpha \approx 131.263°$, so that $m\angle SUB > 60°$. Furthermore, since $m\angle AUB = 60°$ and $m\angle VUS = 60°$, we have that $m\angle AUV = 240° - m\angle SUB = 120° - \alpha \approx 108.737°$, so that $m\angle AUV > 60°$.

We also have that $m\angle USW = 2 \cdot m\angle USD = 2(90° - \alpha) = 180° - 2\alpha \approx 157.473°$, so that $m\angle USW > 60°$. Furthermore, since $m\angle USR = 60°$ and $m\angle TSW = 60°$, we have that $m\angle RST = 240 - m\angle USW = 60° + 2\alpha \approx 82.527°$, so that $m\angle RST > 60°$. □

Lemma A.5.2. *The disjoint components of the "outward" inverter gadget are greater than unit distance apart.*

Proof. We must check distances between the walls and inner structures of the gadget. Because we have that $\alpha > 0°$, all parts of the inner structure are strictly farther from the bottom wall of the gadget than the bottom of the left wire gadget, and thus, we do not need to check for distances between the inner structure and the bottom wall of the gadget.

Meanwhile, because $\tan 0° < \tan \alpha < \tan 60°$, the slope of $\overleftrightarrow{VR}$ is less than that of $\overleftrightarrow{MC}$, and greater than $\overleftrightarrow{MP}$. Thus, given the relative positions of parts of the gadget, it suffices to show that P is greater than unit distance from $\overline{VR}$ and that V is greater than unit distance from either $\overline{MC}$ or $\overline{MP}$.

To accomplish this, we will calculate the positions of points in a Cartesian coordinate system. By fixing the origin $(0, 0)$ to O (note that O is a point in the "tunnel lattice"), we can calculate the Cartesian coordinates of other points from their horizontal and vertical displacement from O using the triangular grid, our earlier shift calculations from Lemma A.2.4, and trigonometry. Since the distance from a point to a line can only be greater than the distance from the point to the segment's corresponding line, this is the calculation we use below.

First, by construction, we have that $U = (1 - \kappa, \frac{\sqrt{3}}{2})$. Additionally, because they lie on the "tunnel grid", we can easily find that $M = (1, 3\sqrt{3})$ and $P = (8, 3\sqrt{3})$. Finally, because $m\angle VUS = 60°$, we have that $m\angle VUD = \alpha + 60°$. Thus, using right triangle trigonometry and the fact that $UV = 2$, we can find the location of V relative to U, to get $V = \left(1 - \kappa + 2\cos(\alpha + 60°), \frac{\sqrt{3}}{2} + 2\sin(\alpha + 60°)\right)$.

Next, we note that the slopes of $\overleftrightarrow{VR}$, $\overleftrightarrow{CM}$, and $\overleftrightarrow{MP}$ are $\tan \alpha$, $\tan 60° = \sqrt{3}$, and $\tan 0° = 0$, respectively. Using this, we can solve for the equations of $\overleftrightarrow{VR}$, $\overleftrightarrow{CM}$, and $\overleftrightarrow{MP}$.

Finally, using the formula for distance between a point and a line, we find that the distance between P and $\overleftrightarrow{VR}$ is $\frac{-(\sqrt{69}+27)\cdot\left(\sqrt{-2(9\sqrt{69}-83)}\cdot(21\sqrt{23}+31\sqrt{3})-4(18\sqrt{23}+113\sqrt{3})\right)}{15840} \approx 1.117$, so that

they are greater than 1 unit apart. We also find that the distance between V and MC is $\frac{-(2)\sqrt{-6(9\sqrt{69}-83)}+9(3\sqrt{23}-13\sqrt{3})}{36} \approx 1.642$, so that they are greater than 1 unit apart. Lastly, we find that the distance between V and $\overleftrightarrow{MP}$ is $\frac{-\sqrt{-6(9\sqrt{69}-83)}}{36} - \frac{\sqrt{23}-21\sqrt{3}}{12} \approx 2.436$, so that they are greater than 1 unit apart. □

A.5.2 The "Inward" Configuration

Now, we examine the "inward" configuration of the inverter gadget in a very similar fashion (see Figure A.9). We will first check angles before checking distances between the walls and inner structures of the gadget.

Lemma A.5.3. *The angles between adjacent components of the "inward" inverter gadget are all greater than* $60°$.

Proof. As before, we begin by overlaying the gadget on top of the "tunnel lattice", like in Figure A.9a. We only focus our analysis on the left side of the gadget since the right side is a mirror image of the left side. Refer to Figure A.9b (a close-up of the region outlined in purple in A.9a) for the following.

As before,we begin by calculating $\theta = m\angle S'U'D'$. By construction, we have that $U'D' = \frac{19}{2} - \kappa$ and that $U'S' = 18$ (note that $\overleftrightarrow{D'S'}$ splits the gadget in half). Thus, $\theta = \cos^{-1}(\frac{\frac{19}{2}-\kappa}{18}) \approx 58.717°$.

Since the left wire's "wire grid" is only horizontally shifted from the tunnel grid, we have that $m\angle B'U'D' = 120°$. It follows that $m\angle S'U'B' = 120° + \theta \approx 178.717°$, so that $m\angle S'U'B' > 60°$. Furthermore, since $m\angle A'U'B' = 60°$ and $m\angle V'U'S' = 60°$, we have that $m\angle A'U'V' = 240° - m\angle S'U'B' = 120° - \theta \approx 61.283°$, so that $m\angle A'U'V' > 60°$.

We also have that $m\angle U'S'W' = 2 \cdot m\angle U'S'D' = 2(90° - \theta) = 180° - 2\theta \approx 62.565°$, so that $m\angle U'S'W' > 60°$. Furthermore, since $m\angle U'S'R' = 60°$ and $m\angle T'S'W' = 60°$, we have that $m\angle R'S'T' = 240 - m\angle U'S'W' = 60° + 2\theta \approx 177.435°$, so that $m\angle R'S'T' > 60°$. □

Lemma A.5.4. *The disjoint components of the "inward" inverter gadget are greater than unit distance apart.*

Proof. We again check distances between the walls and inner structures of the gadget. Again, because we have that $\theta > 0°$, all parts of the inner structure are strictly farther from the bottom wall of the gadget than the bottom of the left wire gadget, and thus, we do not need to check for distances between the inner structure and the bottom wall of the gadget.

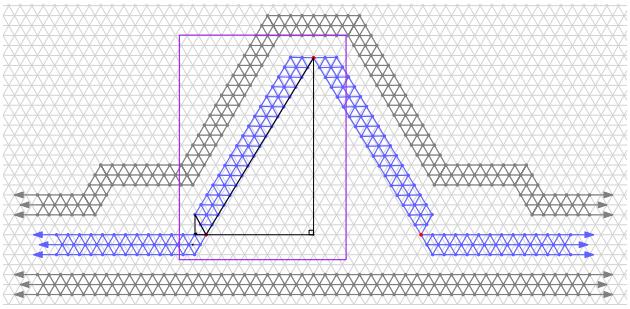

(a)

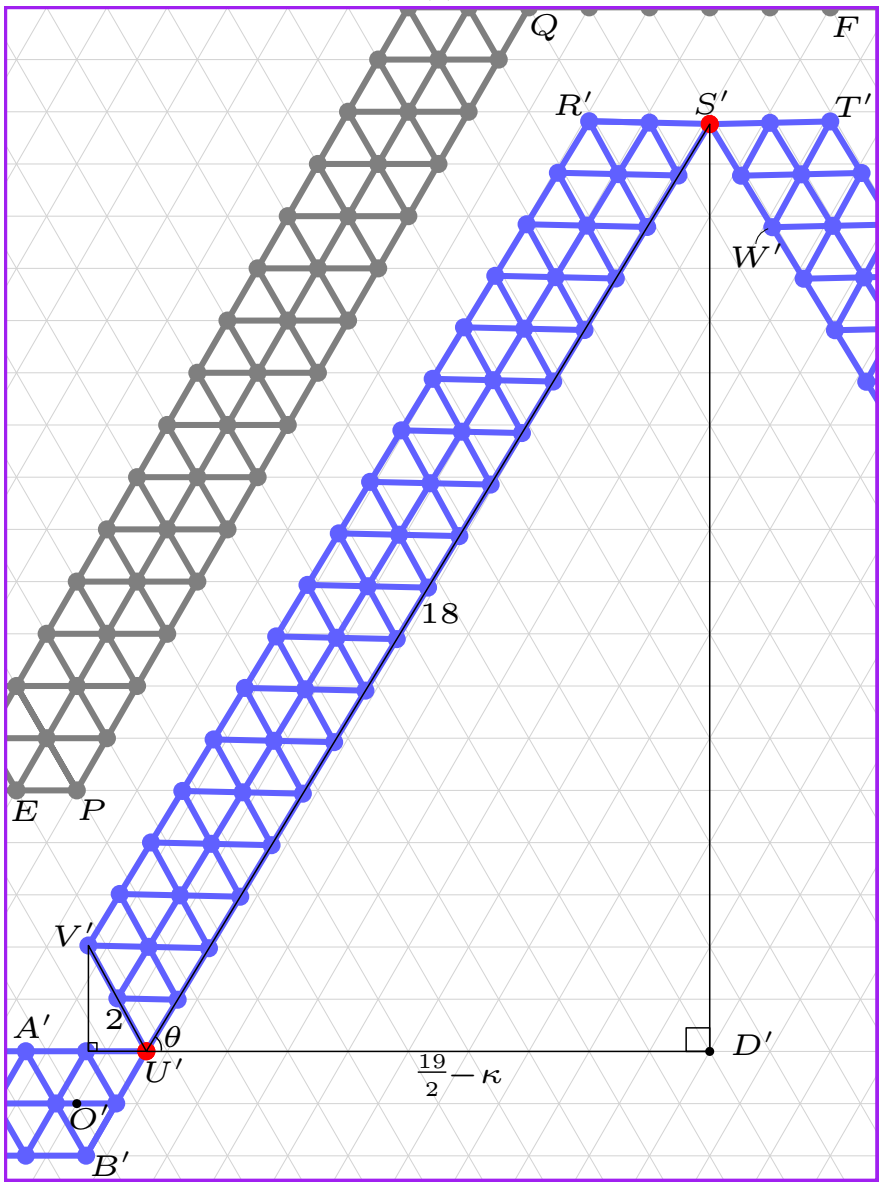

(b)

Figure A.9: The "Inward" Inverter Gadget. (a) The "Inward" Inverter Gadget overlaid on the triangular grid of the tunnel. (b) Close-up of the relevant parts of the gadget.

Meanwhile, because $\tan 0° < \tan\theta < \tan 60°$, the slope of $\overleftrightarrow{V'R'}$ is less than that of $\overleftrightarrow{PQ}$ and greater than that of $\overleftrightarrow{QF}$ (which is parallel to $\overleftrightarrow{EP}$). Also, because $m\angle S'U'D' < m\angle R'S'U'$ ($\theta < 60°$), and because $\overleftrightarrow{QF} \parallel \overleftrightarrow{U'D'}$, we have that the slope of $\overleftrightarrow{RS}$ is less than that of $\overleftrightarrow{QF}$. Thus, given the relative positions of parts of the gadget, it suffices to show that P is greater than unit distance from $\overline{V'R'}$, V' is greater than unit distance from $\overline{EP}$, and R' is greater than unit distance from $\overline{QF}$.

As before, we will check distances by calculating the positions of points in a Cartesian coordinate system. By fixing the origin (0, 0) to O' (note that O' is a point in the "tunnel lattice"), we can calculate the Cartesian coordinates of other points from their horizontal and vertical displacement from O' using the triangular grid, our earlier shift calculations from Lemma A.2.4, and trigonometry.

First, by construction, we have that $U' = (1+\kappa, \frac{\sqrt{3}}{2})$. Additionally, because they all lie on the "tunnel grid", we can easily find that $E = (-1, 3\sqrt{3})$, $P = (0, 3\sqrt{3})$, $Q = (\frac{15}{2}, \frac{21\sqrt{3}}{2})$, and $F = (\frac{25}{2}, \frac{21\sqrt{3}}{2})$. Next, because $m\angle V'U'S' = 60°$, we have that $m\angle V'U'A' = 120° - \theta$. Thus, using right triangle trigonometry and the fact that $U'V' = 2$, we can find the location of V' relative to U', to get $V' = \Big(1 + \kappa - 2\cos(120° - \theta), \frac{\sqrt{3}}{2} + 2\sin(120° - \theta)\Big)$. Finally, because we know that $\overleftrightarrow{V'R'} \parallel \overleftrightarrow{U'S'}$ and that $V'R' = 16$, we can use trigonometry to calculate the position of R' relative to V', to find that $R' = \Big(1 + \kappa - 2\cos(120° - \theta) + 16\cos\theta, \frac{\sqrt{3}}{2} + 2\sin(120° - \theta) + 16\sin\theta\Big)$.

Next, we note that the slopes of $\overleftrightarrow{V'R'}$, $\overleftrightarrow{EP}$, and $\overleftrightarrow{QF}$ are $\tan\theta$, $\tan 0° = 0$, and $\tan 0° = 0$, respectively. Using this, we can solve for the equations of $\overleftrightarrow{V'R'}$, $\overleftrightarrow{EP}$, and $\overleftrightarrow{QF}$.

Finally, using the formula for distance between a point and a line, we find that the distance between P and $\overleftrightarrow{V'R'}$ is $\frac{-(\sqrt{69}-27)\cdot\left(\sqrt{2(9\sqrt{69}+83)}\cdot(21\sqrt{23}-31\sqrt{3})-4(18\sqrt{23}-113\sqrt{3})\right)}{15840} \approx 1.502$, so that they are greater than 1 unit apart. We also find that the distance between V' and EP is $\frac{\sqrt{23}+21\sqrt{3}}{12} - \frac{\sqrt{6(9\sqrt{69}+83)}}{36} \approx 2.576$, so that they are greater than 1 unit apart. Lastly, we find that the distance between R' and $\overleftrightarrow{QF}$ is $\frac{\sqrt{23}+111\sqrt{3}}{12} - \frac{17\sqrt{6(9\sqrt{69}+83)}}{36} \approx 1.893$, so that they are greater than 1 unit apart. □

A.5.3 The Invalid Configurations

Now, we examine the two invalid configurations of the inverter gadget and verify that they are, in fact, not realizable.

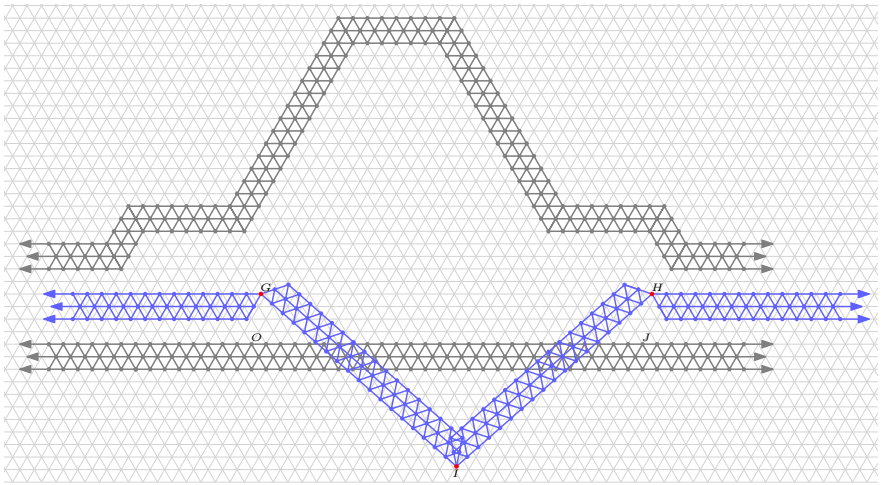

(a)

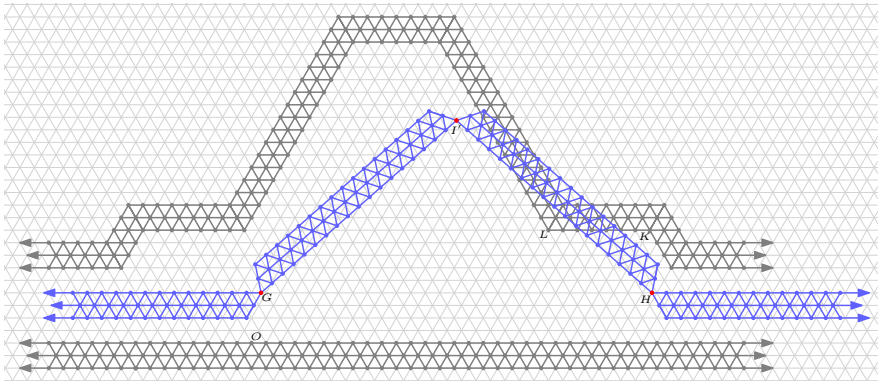

(b)

Figure A.10: The Invalid Configurations (a) The 'Downward" Invalid Configuration (b) The 'Upward' Invalid Configuration

Lemma A.5.5. *The two invalid configurations of the inverter gadget cannot be realized within the problem constraints.*

Proof. We will show that these two configurations force intersections of disks, by showing that the 'downward' configuration forces $\overline{IH}$ to intersect $\overline{OJ}$ and that the 'upward' configuration forces $\overline{I'H}$ to intersect $\overline{LK}$. Note that, while the two inner blue structures can flip about $\overline{GI}$ and $\overline{HI}$, or $\overline{GI'}$ and $\overline{HI'}$, respectively, the locations of G, H, I, and I' are fixed, so that the aforementioned intersections are unavoidable.

To accomplish this, we will calculate the positions of points in a Cartesian coordinate system. By fixing the origin $(0, 0)$ to O (note that O is a point in the "tunnel lattice"), we can calculate the Cartesian coordinates of other points from their horizontal and vertical displacement from O using the triangular grid, our shift calculations from Lemma A.2.4, and trigonometry.

First, we consider the 'downward' configuration in Figure A.10a. By construction, we have that $J = (27, 0)$, $G = (\frac{1}{2} + \kappa, 2\sqrt{3})$, and $H = (\frac{55}{2} + \kappa, 2\sqrt{3})$. Since $GI = HI = 18$, by the Pythagorean Theorem, we find that $I = (14 + \kappa, 2\sqrt{3} - \frac{9\sqrt{7}}{2})$. Clearly, we have that $\overleftrightarrow{OJ}$ is the line $y = 0$. Since the y-coordinate of G is $2\sqrt{3} > 0$ and the y-coordinate of I is $2\sqrt{3} - \frac{9\sqrt{7}}{2} \approx -8.442$, so that it is less than 0, we must have that $\overline{GI}$ intersects the line $y = 0$, so that it intersects $\overleftrightarrow{OJ}$. Furthermore, since the x-coordinate of G is $\frac{1}{2} + \kappa \approx 0.653$, and the x-coordinate of I is $14 + \kappa = 14.153$, both values between 0 and 27, we have that $\overline{GI}$ intersects $\overline{OJ}$ which means that this configuration cannot be realized within the problem constraints.

Next, we consider the 'upward' configuration in Figure A.10b. By construction, we have that $G = (\frac{1}{2} + \kappa, 2\sqrt{3})$, $H = (\frac{55}{2} + \kappa, 2\sqrt{3})$, $L = (\frac{41}{2}, \frac{9\sqrt{3}}{2})$, and $K = (\frac{55}{2}, \frac{9\sqrt{3}}{2})$. Since $GI' = HI' = 18$, by the Pythagorean Theorem, we find that $I' = (14+\kappa, 2\sqrt{3}+\frac{9\sqrt{7}}{2})$. Clearly, we have that $\overleftrightarrow{LK}$ is the line $y = \frac{9\sqrt{3}}{2}$. We can find the equation for $\overleftrightarrow{HI'}$ and plug in $y = \frac{9\sqrt{3}}{2}$ to find that it intersects $\overleftrightarrow{LK}$ at $(\frac{55}{2} + \kappa - \frac{15\sqrt{21}}{14}, \frac{9\sqrt{3}}{2})$. As $(\frac{55}{2} + \kappa - \frac{15\sqrt{21}}{14} \approx 22.743$ is between $\frac{41}{2}$ and $\frac{55}{2}$ (the s-coordinates of L and K, respectively), we thus have that $\overline{I'H}$ intersects $\overline{LK}$, so that this configuration is not realizable within the problem constraints. □

A.6 The Clause Gadget

Our analysis of this gadget will be split into four parts, one for each of the possible configurations of this gadget that we will encounter. Recall that we previously argued that the clause gadget need only handle the cases where 0 or 1 literals are 'true', so that it suffices to only analyze these four configurations.

First, we will argue that the unsatisfied configuration (where all literals have a value of 'false') is truly impossible to realize. Then, we will address each of the three satisfied configurations (where exactly one literal has a value of 'true' and the other two a value of 'false') in turn, showing that each can actually be realized within the constraints of the problem. Note that these have been arbitrarily numbered to distinguish different configurations.

Note that we need not check the distances between the inner structures of this gadget and the outer walls, since the outer walls can be arbitrarily moved outward (while maintaining rigidity and staying on the "tunnel grid") if needed without changing the validity of this gadget.

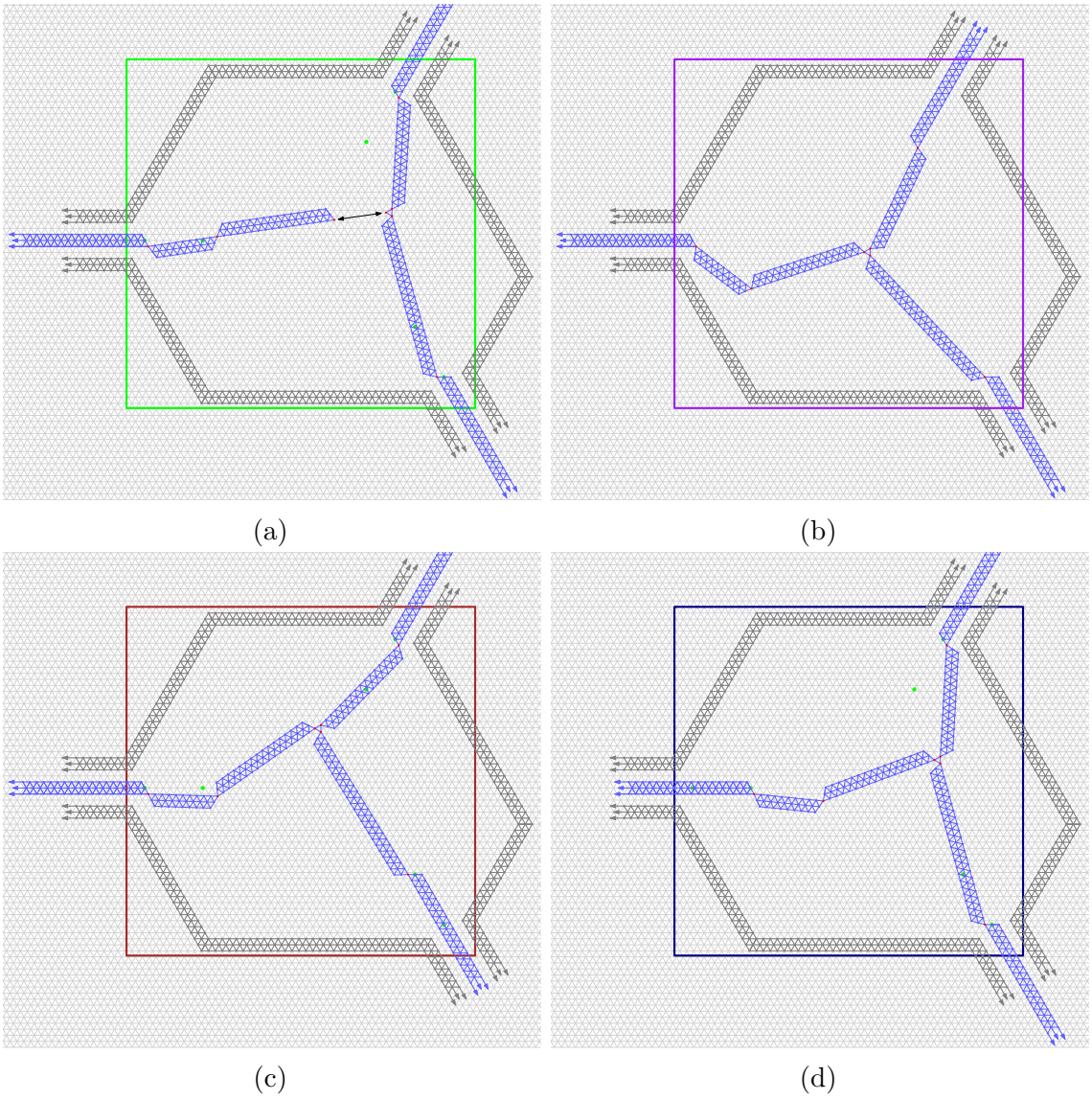

Figure A.11: The Clause Gadget. Each of the following configurations is overlaid onto the tunnel lattice(a) The Unsatisfied Configuration (literal values: FFF) (b) Satisfied Configuration 1 (literal values: TFF) (c) Satisfied Configuration 2 (literal values: TFT) (d) Satisfied Configuration 3 (literal values: FFT)

A.6.1 The Unsatisfied Configuration

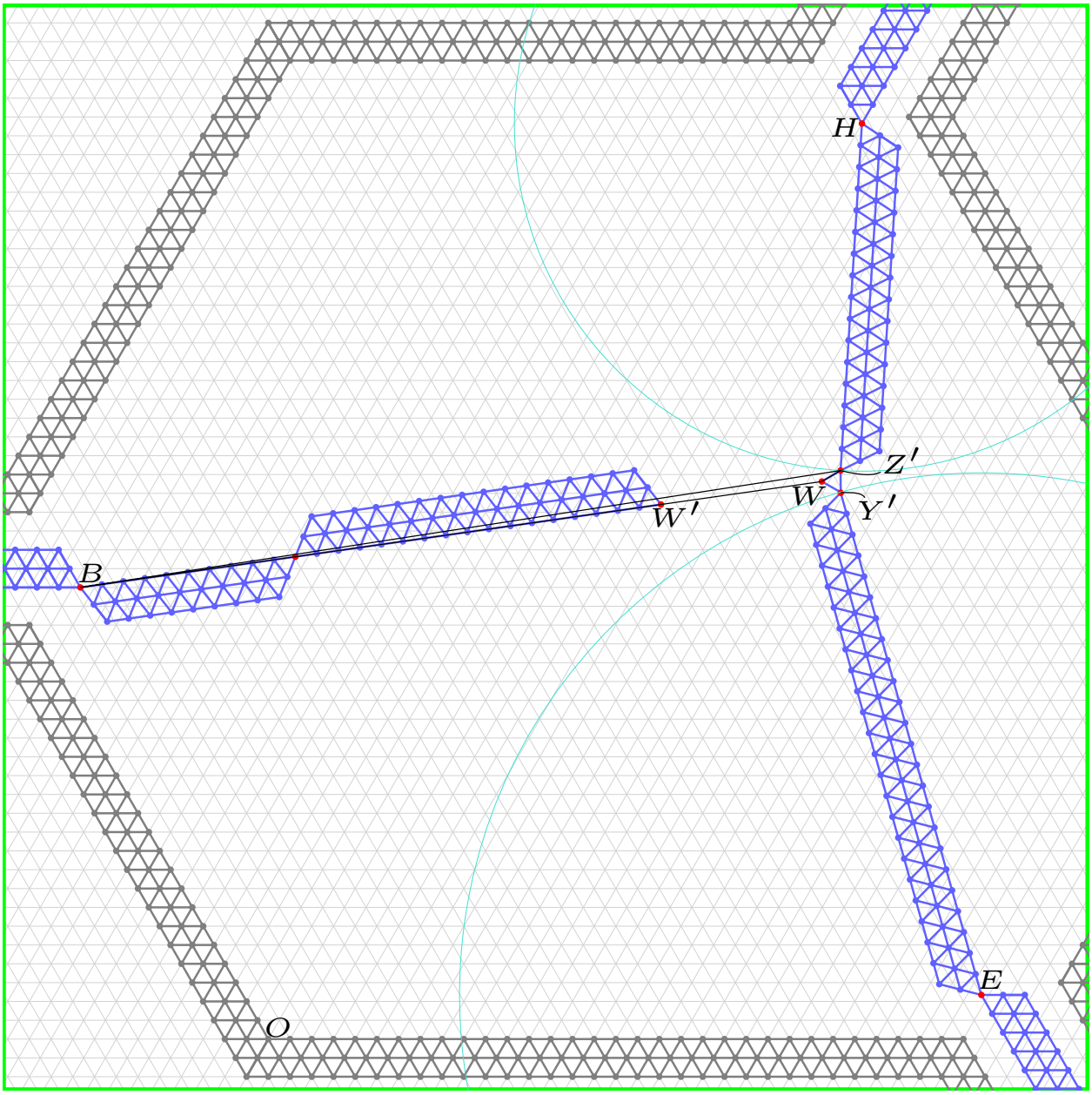

Figure A.12: The Unsatisfied Configuration, a closeup of the relevant parts of Figure A.11a

Let us begin by analyzing the unsatisfied configuration of the gadget. Notice that we already overlaid the gadget onto the "tunnel lattice" in Figure A.11a.

Lemma A.6.1. *The unsatisfied configuration cannot be realized as a valid configuration of the clause gadget.*

Proof. We will show that this configuration cannot have W coincide with W'. Note that, while the inner blue structures can flip about $\overline{HZ'}, \overline{EY'}$ and $\overline{BW'}$, respectively, the distances HZ', EY', and BW' are fixed (or rather bounded in the case of BW'), so that the aforementioned co-incidence is impossible.

Since this gadget has the most internal moving parts, calculating the angles between its inner structures will require us to know the relative positions of some of the points in Figure A.13 (a close-up of the region outlined in green in A.11a).

To accomplish this, we will calculate the positions of points in a Cartesian coordinate system. By fixing the origin $(0, 0)$ to O (note that O is a point in the "tunnel lattice"), we can calculate the Cartesian coordinates of other points from their horizontal and vertical displacement from O using the triangular grid, our shift calculations from A.2.4, algebra, and trigonometry. Once we know the coordinates of three points, we can use simple trigonometry to find the angle formed between them.

First, by construction, we find that

$$B = \left(-\frac{17}{2} - \kappa, 12\sqrt{3}\right), E = \left(\frac{131}{4} + \frac{\kappa}{2}, \frac{5\sqrt{3}}{4} - \frac{\kappa\sqrt{3}}{2}\right), \text{ and } H = \left(\frac{109}{4} + \frac{\kappa}{2}, \frac{97\sqrt{3}}{4} + \frac{\kappa\sqrt{3}}{2}\right).$$

□

We also know that $HZ' = 16$, $EY' = 24$ and that the maximum distance for BW' is 27. Now, rather that trying to prove that W can only be greater that 27 units from B, we argue that Z' can only be greater than 28 units away from B, because $WZ' = 1$, and by the triangle inequality, $BZ' \leq BW + 1$, so that $BZ' > 28 \implies BW + 1 > 28 \implies BW > 27$.

We try to find the closest possible position of Z' to B, noting that $HZ' = 16$ and $EZ' < 25$ (because $Y'Z' = 1$). If we let $Z' = (x, y)$, Then we are trying to solve

$$\min\left(\sqrt{\left(x - \left(-\frac{17}{2} - \kappa\right)\right)^2 + \left(y - \left(12\sqrt{3}\right)\right)^2}\right)$$

$$\text{such that } \begin{cases} \sqrt{\left(x - \left(\frac{109}{4} + \frac{\kappa}{2}\right)\right)^2 + \left(y - \left(\frac{97\sqrt{3}}{4} + \frac{\kappa\sqrt{3}}{2}\right)\right)^2} = 16 \\ \sqrt{\left(x - \left(\frac{131}{4} + \frac{\kappa}{2}\right)\right)^2 + \left(y - \left(\frac{5\sqrt{3}}{4} - \frac{\kappa\sqrt{3}}{2}\right)\right)^2} \leq 25 \end{cases}$$

Solving this (using computer-aided methods), we find that the minimum distance from B to Z' is approximately 35.373 units, when $(x, y) \approx (26.308, 26.168)$, which is clearly greater that

28 units. Thus, by our earlier argument, we have that W and W' cannot coincide, so that this configuration is not possible within our problem constraints.

A.6.2 Satisfied Configuration 1

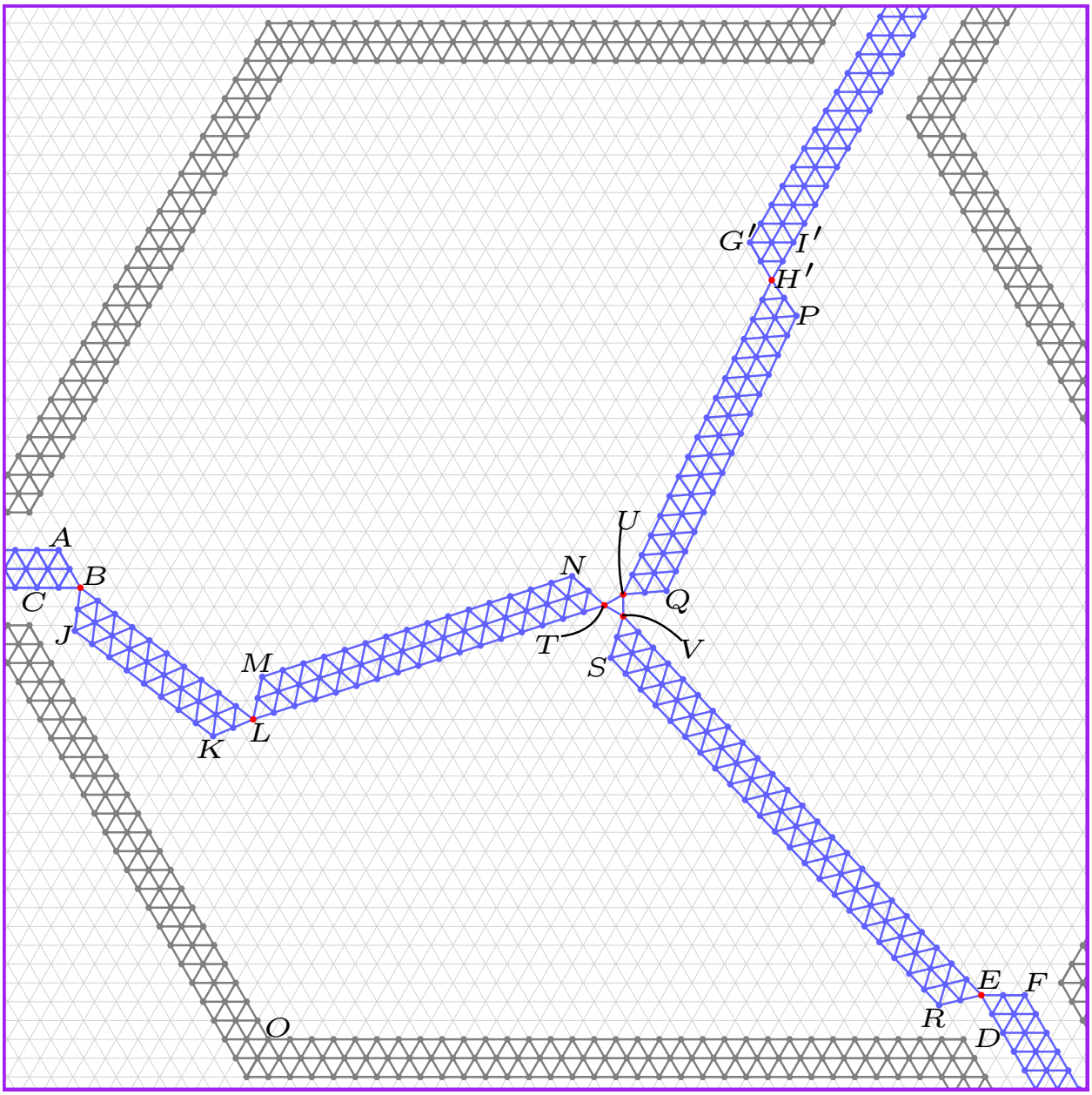

Figure A.13: Satisfied Configuration 1, a closeup of the relevant parts of Figure A.11b

Now, we analyze one of the satisfied configuration of the gadget. Notice that we already overlaid the gadget onto the "tunnel lattice" in Figure A.11a.

Lemma A.6.2. *The angles between adjacent components of satisfied configuration 1 of the clause gadget are all greater than* $60°$.

Proof. Since this gadget has the most internal moving parts, calculating the angles between its inner structures will require us to know the relative positions of some of the points in Figure A.13 (a close-up of the region outlined in purple in A.11b).

To accomplish this, we will calculate the positions of points in a Cartesian coordinate system. By fixing the origin $(0, 0)$ to O (note that O is a point in the "tunnel lattice"), we can calculate the Cartesian coordinates of other points from their horizontal and vertical displacement from O using the triangular grid, our shift calculations from A.2.4, algebra, and trigonometry. Once we know the coordinates of three points, we can use simple trigonometry to find the angle formed between them.

First, by construction, we find that

$$A = \left(-\frac{19}{2} - \kappa, 13\sqrt{3}\right), B = \left(-\frac{17}{2} - \kappa, 12\sqrt{3}\right),$$
$$E = \left(\frac{131}{4} + \frac{\kappa}{2}, \frac{5\sqrt{3}}{4} - \frac{\kappa\sqrt{3}}{2}\right), F = \left(\frac{139}{4} + \frac{\kappa}{2}, \frac{5\sqrt{3}}{4} - \frac{\kappa\sqrt{3}}{2}\right),$$
$$G' = \left(\frac{89}{4} - \frac{\kappa}{2}, \frac{85\sqrt{3}}{4} - \frac{\kappa\sqrt{3}}{2}\right), \text{ and } H' = \left(\frac{93}{4} - \frac{\kappa}{2}, \frac{81\sqrt{3}}{4} - \frac{\kappa\sqrt{3}}{2}\right).$$

Next, using the coordinates for E and H', and the fact that $EV = 24$ and $H'U = 16$, we can solve for the coordinates of V, $V = (x_1, y_1)$, given that we want U to be a unit vertically above V, $U = (x_1, y_1 + 1)$, using the following system of equations

$$\begin{cases} \sqrt{\left(x_1 - \left(\frac{131}{4} + \frac{\kappa}{2}\right)\right)^2 + \left(y_1 - \left(\frac{5\sqrt{3}}{4} - \frac{\kappa\sqrt{3}}{2}\right)\right)^2} = 24 \\ \sqrt{\left(x_1 - \left(\frac{93}{4} - \frac{\kappa}{2}\right)\right)^2 + \left(y_1 + 1 - \left(\frac{81\sqrt{3}}{4} - \frac{\kappa\sqrt{3}}{2}\right)\right)^2} = 16 \end{cases}$$

Of the two sets of solutions to this system, we choose the one with the lower value for x_1, as this matches our construction. We get that $x_1 \approx 16.340, y_1 \approx 19.474$ (the exact solution is too long to display on the page).

As mentioned before, we have that $V = (x_1, y_1)$ and $U = (x_1, y_1 + 1)$, but we also have that $T = (x_1 - \frac{\sqrt{3}}{2}, y_1 + \frac{1}{2})$. Now, using this and the coordinates of B, and the fact that $BL = 10$

and $LT = 17$, we can solve for the coordinates of L, $L = (x_2, y_2)$ using the following system of equations

$$\begin{cases} \sqrt{\left(x_2 - \left(-\frac{17}{2} - \kappa\right)\right)^2 + \left(y_2 - \left(12\sqrt{3}\right)\right)^2} = 10 \\ \sqrt{\left(x_2 - \left(x_1 - \frac{\sqrt{3}}{2}\right)\right)^2 + \left(y_2 - \left(y_1 + \frac{1}{2}\right)\right)^2} = 17 \end{cases}$$

Of the two sets of solutions to this system, we choose the one with the lower value for y_2, as this matches our construction. We get that $x_2 \approx -0.696, y_2 \approx 14.728$ (again, the exact solution is too long to display on the page).

Now, using all of our computed coordinates for points, we can use the law of cosines to find angles. Namely, given the coordinates of the points X, Y, and Z, we can find $m\angle XYZ$ as follows: letting D_{XY}, D_{YZ}, and D_{XZ} be the Euclidean distance between points X and Y, Y and Z, and X and Z, respectively, we have that $m\angle XYZ = \cos^{-1}(\frac{D_{XY}^2 + D_{YZ}^2 - D_{XZ}^2}{2 \cdot D_{XY} \cdot D_{YZ}})$. Note that because of the length of exactly-valued expressions, we only give approximate measures of all angles.

Using this, we find that $m\angle FEV \approx 133.387°$, so that $m\angle FEV > 60°$. Since $m\angle REV = m\angle DEF = 60°$, we have that $m\angle RED = 240° - m\angle FEV \approx 106.613°$, so that $m\angle RED > 60°$.

We find that $m\angle G'H'U \approx 124.719°$, so that $m\angle G'H'U > 60°$. Since $m\angle PH'U = m\angle G'H'I' = 60°$, we have that $m\angle I'H'P = 240° - m\angle G'H'U \approx 115.281°$, so that $m\angle I'H'P' > 60°$.

We find that $m\angle ABL \approx 157.276°$, so that $m\angle ABL > 60°$. Since $m\angle ABC = m\angle JBL = 60°$, we have that $m\angle CBJ = 240° - m\angle ABL \approx 82.724°$, so that $m\angle CBJ > 60°$.

We find that $m\angle EVU \approx 136.613°$, so that $m\angle EVU > 60°$. We have that $m\angle H'UV \approx 154.719°$, so that (since $m\angle H'UQ = 60°$) $m\angle QUV = m\angle H'UV - 60° \approx 94.719°$, so that $m\angle QUV > 60°$.

We find that $m\angle H'UT \approx 145.281°$, so that $m\angle H'UT > 60°$. We have that $m\angle LTU \approx 167.973°$, so that (since $m\angle LTN = 60°$) $m\angle NTU = m\angle LTU - 60° \approx 107.973°$, so that $m\angle NTU > 60°$.

We find that $m\angle LTV \approx 132.027°$, so that $m\angle LTV > 60°$. We have that $m\angle EVT \approx 163.387°$, so that (since $m\angle SVE = 60°$) $m\angle SVT = m\angle EVT - 60° \approx 103.387°$, so that $m\angle SVT > 60°$.

Finally, we find that $m\angle BLT \approx 124.751°$. Since $m\angle TLM = 60°$, we have that $m\angle BLM = m\angle BLT - 60° \approx 64.751°$, so that $m\angle BLM > 60°$. Since we also have $m\angle BLK = 60°$, we have that $m\angle KLT = 240° - m\angle BLM \approx 175.249°$, so that $m\angle KLT > 60°$. □

Lemma A.6.3. *The disjoint components of satisfied configuration 1 of the clause gadget are greater than unit distance apart.*

Proof. As previously noted, we do not need to check the distances between the inner structures of this configuration and the outer wall, so that it only remains to check the distances between $\overline{EV}$ and $\overline{QU}$, $\overline{H'U}$ and $\overline{NT}$, and $\overline{LT}$ and $\overline{SV}$, respectively.

However, because we already know that $m\angle EVU + m\angle VUQ \approx 231.331°$, we have that $m\angle EVU + m\angle VUQ > 180°$, so that $\overline{EV}$ and $\overline{QU}$ are closest at $VU = 1$, and the remainder of these line segments are more than unit distance apart. Similarly, because we know that $m\angle H'UT + m\angle UTN \approx 253.254°$, we have that $m\angle H'UT + m\angle UTN > 180°$, so that $\overline{H'U}$ and $\overline{NT}$ are closest at $UT = 1$, and the remainder of these line segments are more than unit distance apart. Finally, because we know that $m\angle LTV + m\angle TVS \approx 235.414°$, we have that $m\angle LTV + m\angle TVS > 180°$, so that $\overline{LT}$ and $\overline{SV}$ are closest at $TV = 1$, and the remainder of these line segments are more than unit distance apart. □

A.6.3 Satisfied Configuration 2

Now, we analyze another one of the satisfied configuration of the gadget. Notice that we already overlaid the gadget onto the "tunnel lattice" in Figure A.11c.

Lemma A.6.4. *The angles between adjacent components of satisfied configuration 2 of the clause gadget are all greater than* $60°$.

Proof. Since this gadget has the most internal moving parts, calculating the angles between its inner structures will require us to know the relative positions of some of the points in Figure A.14 (a close-up of the region outlined in brown in A.11c).

To accomplish this, we will calculate the positions of points in a Cartesian coordinate system. By fixing the origin $(0, 0)$ to O (note that O is a point in the "tunnel lattice"), we can calculate the Cartesian coordinates of other points from their horizontal and vertical displacement from O using the triangular grid, our shift calculations from A.2.4, algebra, and trigonometry. Once we know the coordinates of three points, we can use simple trigonometry to find the angle formed between them.

First, by construction, we find that

$$A = \left(-\frac{19}{2} - \kappa, 13\sqrt{3}\right), B = \left(-\frac{17}{2} - \kappa, 12\sqrt{3}\right),$$
$$E' = \left(\frac{115}{4} - \frac{\kappa}{2}, \frac{21\sqrt{3}}{4} + \frac{\kappa\sqrt{3}}{2}\right), F' = \left(\frac{123}{4} - \frac{\kappa}{2}, \frac{21\sqrt{3}}{4} + \frac{\kappa\sqrt{3}}{2}\right),$$
$$G = \left(\frac{105}{4} + \frac{\kappa}{2}, \frac{101\sqrt{3}}{4} + \frac{\kappa\sqrt{3}}{2}\right), \text{ and } H = \left(\frac{109}{4} + \frac{\kappa}{2}, \frac{97\sqrt{3}}{4} + \frac{\kappa\sqrt{3}}{2}\right).$$

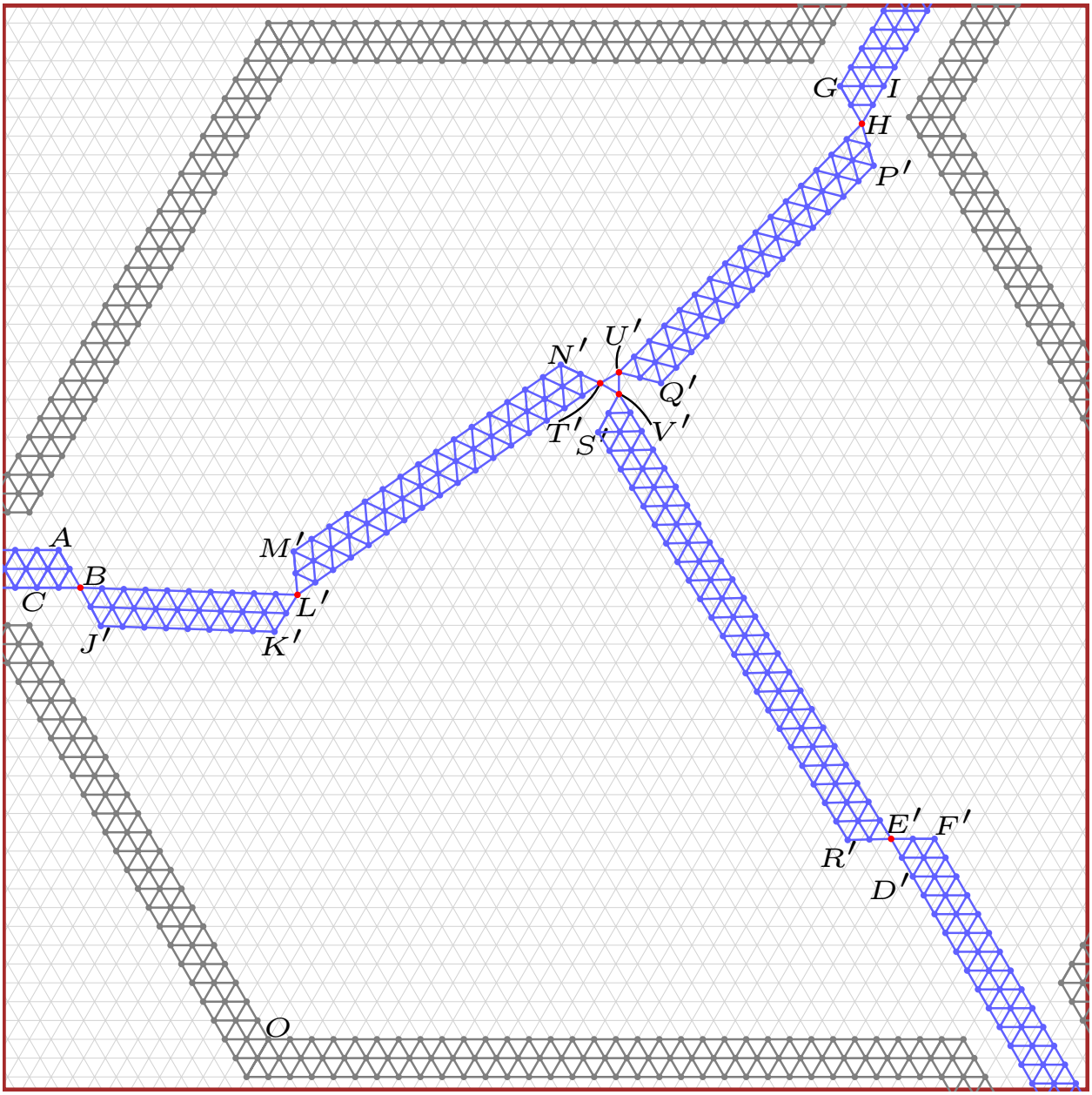

Figure A.14: Satisfied Configuration 2, a closeup of the relevant parts of Figure A.11c

Next, using the coordinates for E' and H, and the fact that $E'V' = 24$ and $HU' = 16$, we can solve for the coordinates of V', $V' = (x_3, y_3)$, given that we want U' to be a unit vertically

above V', $U' = (x_3, y_3 + 1)$, using the following system of equations

$$\begin{cases} \sqrt{\left(x_3 - \left(\frac{115}{4} - \frac{\kappa}{2}\right)\right)^2 + \left(y_3 - \left(\frac{21\sqrt{3}}{4} + \frac{\kappa\sqrt{3}}{2}\right)\right)^2} = 24 \\ \sqrt{\left(x_3 - \left(\frac{109}{4} + \frac{\kappa}{2}\right)\right)^2 + \left(y_3 + 1 - \left(\frac{97\sqrt{3}}{4} + \frac{\kappa\sqrt{3}}{2}\right)\right)^2} = 16 \end{cases}$$

Of the two sets of solutions to this system, we choose the one with the lower value for x_3, as this matches our construction. We get that $x_3 \approx 16.340, y_3 \approx 19.474$ (the exact solution is too long to display on the page).

As mentioned before, we have that $V' = (x_3, y_3)$ and $U' = (x_3, y_3 + 1)$, but we also have that $T' = (x_3 - \frac{\sqrt{3}}{2}, y_3 + \frac{1}{2})$. Now, using this and the coordinates of B, and the fact that $BL' = 10$ and $L'T' = 17$, we can solve for the coordinates of L', $L' = (x_4, y_4)$ using the following system of equations

$$\begin{cases} \sqrt{\left(x_4 - \left(-\frac{17}{2} - \kappa\right)\right)^2 + \left(y_4 - \left(12\sqrt{3}\right)\right)^2} = 10 \\ \sqrt{\left(x_4 - \left(x_3 - \frac{\sqrt{3}}{2}\right)\right)^2 + \left(y_4 - \left(y_3 + \frac{1}{2}\right)\right)^2} = 17 \end{cases}$$

Of the two sets of solutions to this system, we choose the one with the lower value for y_4, as this matches our construction. We get that $x_4 \approx -0.696, y_4 \approx 14.728$ (again, the exact solution is too long to display on the page).

Now, using all of our computed coordinates for points, we can once again use the law of cosines to find angles, by the same method used above. Note that because of the length of exactly-valued expressions, we only give approximate measures of all angles.

Using this, we find that $m\angle F'E'V' \approx 121.478°$, so that $m\angle F'E'V' > 60°$. Since $m\angle R'E'V' = m\angle D'E'F' = 60°$, we have that $m\angle R'E'D' = 240° - m\angle F'E'V' \approx 118.522°$, so that $m\angle R'E'D' > 60°$.

We find that $m\angle GHU' \approx 105.647°$, so that $m\angle GHU' > 60°$. Since $m\angle P'HU' = m\angle GHI = 60°$, we have that $m\angle IHP' = 240° - m\angle GHU' \approx 134.353°$, so that $m\angle IHP'' > 60°$.

We find that $m\angle ABL' \approx 121.885°$, so that $m\angle ABL' > 60°$. Since $m\angle ABC = m\angle J'BL' = 60°$, we have that $m\angle CBJ' = 240° - m\angle ABL' \approx 118.115°$, so that $m\angle CBJ' > 60°$.

We find that $m\angle E'V'U' \approx 148.522°$, so that $m\angle E'V'U' > 60°$. We have that $m\angle HU'V' \approx 135.647°$, so that (since $m\angle HU'Q' = 60°$) $m\angle Q'U'V' = m\angle HU'V' - 60° \approx 75.647°$, so that $m\angle Q'U'V' > 60°$.

We find that $m\angle HU'T' \approx 164.353°$, so that $m\angle HU'T' > 60°$. We have that $m\angle L'T'U' \approx 175.050°$, so that (since $m\angle L'T'N' = 60°$) $m\angle N'T'U' = (360° - m\angle L'T'U') - 60° \approx 124.950°$, so that $m\angle N'T'U' > 60°$.

We find that $m\angle L'T'V' \approx 115.050°$, so that $m\angle L'T'V' > 60°$. We have that $m\angle E'V'T' \approx 151.478°$, so that (since $m\angle S'V'E' = 60°$) $m\angle S'V'T' = m\angle E'V'T' - 60° \approx 91.478°$, so that $m\angle S'V'T' > 60°$.

Finally, we find that $m\angle BL'T' \approx 143.165°$. Since $m\angle T'L'M' = 60°$, we have that $m\angle BL'M' = m\angle BL'T' - 60° \approx 83.165°$, so that $m\angle BL'M' > 60°$. Since we also have $m\angle BL'K' = 60°$, we have that $m\angle K'L'T' = 240° - m\angle BL'M' \approx 156.835°$, so that $m\angle K'L'T' > 60°$. □

Lemma A.6.5. *The disjoint components of satisfied configuration 2 of the clause gadget are greater than unit distance apart.*

Proof. As previously noted, we do not need to check the distances between the inner structures of this configuration and the outer wall, so that it only remains to check the distances between $\overline{E'V'}$ and $\overline{Q'U'}$, $\overline{HU'}$ and $\overline{N'T'}$, and $\overline{L'T'}$ and $\overline{S'V'}$, respectively.

However, because we already know that $m\angle E'V'U' + m\angle V'U'Q' \approx 224.169°$, we have that $m\angle E'V'U' + m\angle V'U'Q' > 180°$, so that $\overline{E'V'}$ and $\overline{Q'U'}$ are closest at $V'U' = 1$, and the remainder of these line segments are more than unit distance apart. Similarly, because we know that $m\angle HU'T' + m\angle U'T'N' \approx 289.303°$, we have that $m\angle HU'T' + m\angle U'T'N' > 180°$, so that $\overline{HU'}$ and $\overline{N'T'}$ are closest at $U'T' = 1$, and the remainder of these line segments are more than unit distance apart. Finally, because we know that $m\angle L'T'V' + m\angle T'V'S' \approx 206.528°$, we have that $m\angle L'T'V' + m\angle T'V'S' > 180°$, so that $\overline{L'T'}$ and $\overline{S'V'}$ are closest at $T'V' = 1$, and the remainder of these line segments are more than unit distance apart. □

A.6.4 Satisfied Configuration 3

Now, we analyze the third of the satisfied configuration of the gadget. Notice that we already overlaid the gadget onto the "tunnel lattice" in Figure A.11d.

Lemma A.6.6. *The angles between adjacent components of satisfied configuration 3 of the clause gadget are all greater than* $60°$.

Proof. Since this gadget has the most internal moving parts, calculating the angles between its inner structures will require us to know the relative positions of some of the points in Figure A.15 (a close-up of the region outlined in navy in A.11d).

To accomplish this, we will calculate the positions of points in a Cartesian coordinate system. By fixing the origin $(0, 0)$ to O (note that O is a point in the "tunnel lattice"), we can calculate the Cartesian coordinates of other points from their horizontal and vertical displacement from O using the triangular grid, our shift calculations from A.2.4, algebra, and trigonometry. Once we know the coordinates of three points, we can use simple trigonometry to find the angle formed between them.

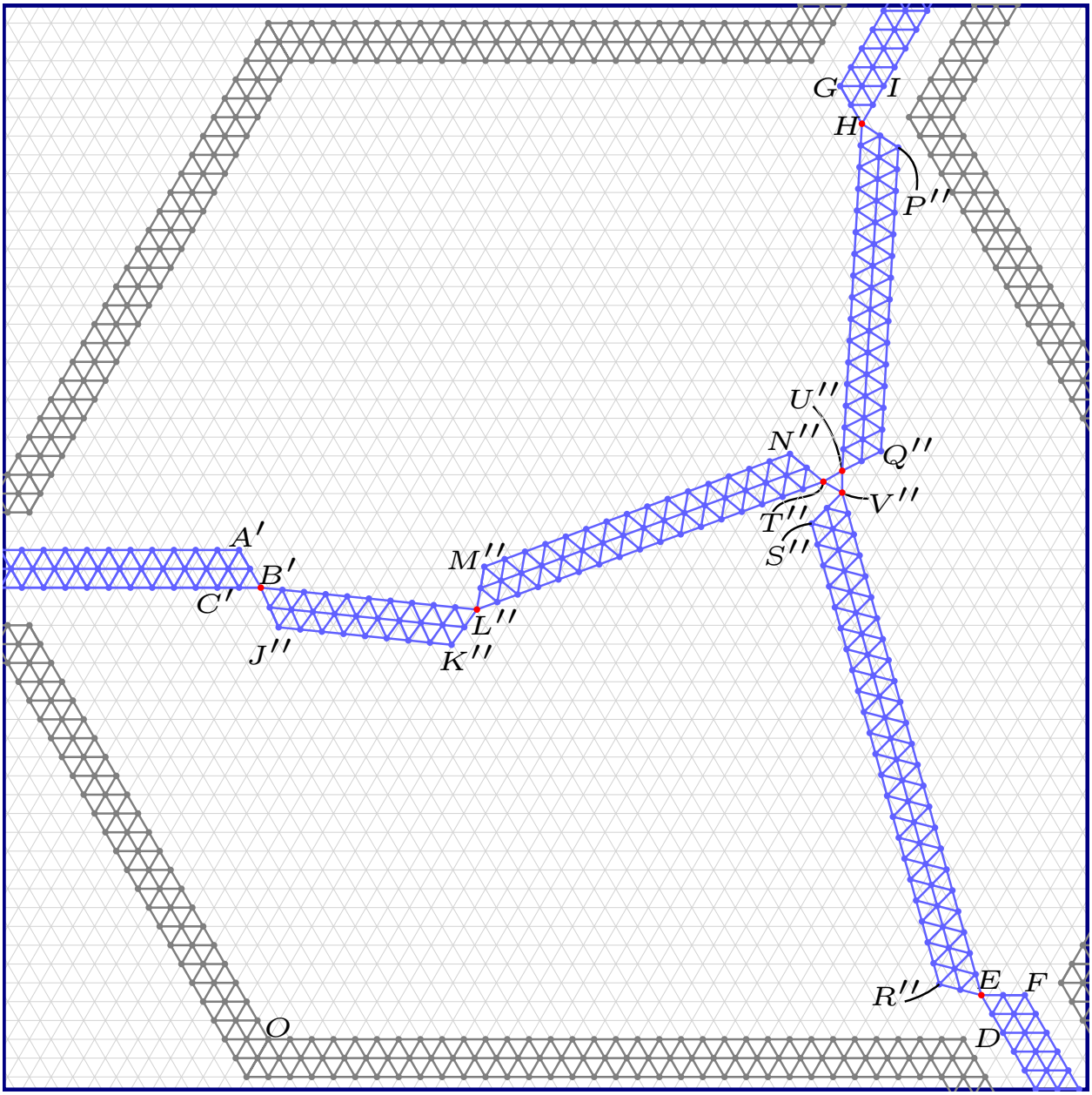

Figure A.15: Satisfied Configuration 3, a closeup of the relevant parts of Figure A.11d

First, by construction, we find that

$$A' = \left(-\frac{3}{2} + \kappa, 13\sqrt{3}\right), B' = \left(-\frac{1}{2} + \kappa, 12\sqrt{3}\right),$$
$$E = \left(\frac{131}{4} + \frac{\kappa}{2}, \frac{5\sqrt{3}}{4} - \frac{\kappa\sqrt{3}}{2}\right), F = \left(\frac{139}{4} + \frac{\kappa}{2}, \frac{5\sqrt{3}}{4} - \frac{\kappa\sqrt{3}}{2}\right),$$
$$G = \left(\frac{105}{4} + \frac{\kappa}{2}, \frac{101\sqrt{3}}{4} + \frac{\kappa\sqrt{3}}{2}\right), \text{ and } H = \left(\frac{109}{4} + \frac{\kappa}{2}, \frac{97\sqrt{3}}{4} + \frac{\kappa\sqrt{3}}{2}\right).$$

Next, using the coordinates for E and H, and the fact that $EV = 24$ and $HU'' = 16$, we can solve for the coordinates of V'', $V'' = (x_5, y_5)$, given that we want U'' to be a unit vertically above V'', $U'' = (x_5, y_5 + 1)$, using the following system of equations

$$\begin{cases} \sqrt{\left(x_5 - \left(\frac{131}{4} + \frac{\kappa}{2}\right)\right)^2 + \left(y_5 - \left(\frac{5\sqrt{3}}{4} - \frac{\kappa\sqrt{3}}{2}\right)\right)^2} = 24 \\ \sqrt{\left(x_5 - \left(\frac{109}{4} + \frac{\kappa}{2}\right)\right)^2 + \left(y_5 + 1 - \left(\frac{97\sqrt{3}}{4} + \frac{\kappa\sqrt{3}}{2}\right)\right)^2} = 16 \end{cases}$$

Of the two sets of solutions to this system, we choose the one with the lower value for x_5, as this matches our construction. We get that $x_5 \approx 16.340, y_5 \approx 19.474$ (the exact solution is too long to display on the page).

As mentioned before, we have that $V'' = (x_5, y_5)$ and $U'' = (x_5, y_5 + 1)$, but we also have that $T'' = (x_5 - \frac{\sqrt{3}}{2}, y_5 + \frac{1}{2})$. Now, using this and the coordinates of B', and the fact that $B'L'' = 10$ and $L''T'' = 17$, we can solve for the coordinates of L'', $L'' = (x_6, y_6)$ using the following system of equations

$$\begin{cases} \sqrt{\left(x_6 - \left(-\frac{1}{2} + \kappa\right)\right)^2 + \left(y_6 - \left(12\sqrt{3}\right)\right)^2} = 10 \\ \sqrt{\left(x_6 - \left(x_5 - \frac{\sqrt{3}}{2}\right)\right)^2 + \left(y_6 - \left(y_5 + \frac{1}{2}\right)\right)^2} = 17 \end{cases}$$

Of the two sets of solutions to this system, we choose the one with the lower value for y_6, as this matches our construction. We get that $x_6 \approx -0.696, y_6 \approx 14.728$ (again, the exact solution is too long to display on the page).

Now, using all of our computed coordinates for points, we can once again use the law of cosines to find angles, by the same method used above. Note that because of the length of exactly-valued expressions, we only give approximate measures of all angles.

Using this, we find that $m\angle FEV'' \approx 105.487°$, so that $m\angle FEV'' > 60°$. Since $m\angle R''EV'' = m\angle DEF = 60°$, we have that $m\angle R''ED = 240° - m\angle FEV'' \approx 134.513°$, so that $m\angle R''ED > 60°$.

We find that $m\angle GHU'' \approx 146.744°$, so that $m\angle GHU'' > 60°$. Since $m\angle P''HU'' = m\angle GHI = 60°$, we have that $m\angle IHP'' = 240° - m\angle GHU'' \approx 93.256°$, so that $m\angle IHP''' > 60°$.

We find that $m\angle A'B'L'' \approx 125.780°$, so that $m\angle A'B'L'' > 60°$. Since $m\angle A'B'C' = m\angle J''B'L'' = 60°$, we have that $m\angle C'B'J'' = 240° - m\angle A'B'L'' \approx 114.220°$, so that $m\angle C'B'J'' > 60°$.

We find that $m\angle EV''U'' \approx 164.513°$, so that $m\angle EV''U'' > 60°$. We have that $m\angle HU''V'' \approx 176.744°$, so that (since $m\angle HU''Q'' = 60°$) $m\angle Q''U''V'' = m\angle HU''V'' - 60° \approx 116.744°$, so that $m\angle Q''U''V'' > 60°$.

We find that $m\angle HU''T'' \approx 123.256°$, so that $m\angle HU''T'' > 60°$. We have that $m\angle L''T''U'' \approx 170.248°$, so that (since $m\angle L''T''N'' = 60°$) $m\angle N''T''U'' = m\angle L''T''U'' - 60° \approx 110.248°$, so that $m\angle N''T''U'' > 60°$.

We find that $m\angle L''T''V'' \approx 129.752°$, so that $m\angle L''T''V'' > 60°$. We have that $m\angle EV''T'' \approx 135.487°$, so that (since $m\angle S''V''E = 60°$) $m\angle S''V''T'' = m\angle EV''T'' - 60° \approx 75.487°$, so that $m\angle S''V''T'' > 60°$.

Finally, we find that $m\angle B'L''T'' \approx 153.972°$. Since $m\angle T''L''M'' = 60°$, we have that $m\angle B'L''M'' = m\angle B'L''T'' - 60° \approx 93.972°$, so that $m\angle B'L''M'' > 60°$. Since we also have $m\angle B'L''K'' = 60°$, we have that $m\angle K''L''T'' = 240° - m\angle B'L''M'' \approx 146.028°$, so that $m\angle K''L''T'' > 60°$. □

Lemma A.6.7. *The disjoint components of satisfied configuration 3 of the clause gadget are greater than unit distance apart.*

Proof. As previously noted, we do not need to check the distances between the inner structures of this configuration and the outer wall, so that it only remains to check the distances between $\overline{EV''}$ and $\overline{Q''U''}$, $\overline{HU''}$ and $\overline{N''T''}$, and $\overline{L''T''}$ and $\overline{S''V''}$, respectively.

However, because we already know that $m\angle EV''U'' + m\angle V''U''Q'' \approx 281.257°$, we have that $m\angle EV''U'' + m\angle V''U''Q'' > 180°$, so that $\overline{EV''}$ and $\overline{Q''U''}$ are closest at $V''U'' = 1$, and the remainder of these line segments are more than unit distance apart. Similarly, because we know that $m\angle HU''T'' + m\angle U''T''N'' \approx 233.503°$, we have that $m\angle HU''T'' + m\angle U''T''N'' > 180°$, so that $\overline{HU''}$ and $\overline{N''T''}$ are closest at $U''T'' = 1$, and the remainder of these line segments are more than unit distance apart. Finally, because we know that $m\angle L''T''V'' + m\angle T''V''S'' \approx 205.240°$, we have that $m\angle L''T''V'' + m\angle T''V''S'' > 180°$, so that $\overline{L''T''}$ and $\overline{S''V''}$ are closest at $T''V'' = 1$, and the remainder of these line segments are more than unit distance apart. □